Nuclear Structure and Saturation Properties Around ^{48}Ca

Andrea Gottardo

INFN-LNL, Italy

On behalf of the E786S collaboration

Index

- Saturation properties of nuclei
  - liquid drop, charge radii
  - charge density bubbles
- The puzzling case of ^{46}Ar
  - N=28
  - small B(E2)
  - Coulex and (p,p')
- The direct proton transfer reaction ^{46}Ar(^{3}He,d)^{47}K
  - motivation
  - AGATA-MUGAST-VAMOS-HeCTOR
  - data analysis
- Results compared to theoretical models
- Future perspectives

Daniele Brugnara PhD work
Recipient of the 2023 INFN Villi Award
for the best thesis in nuclear physics in Italy

Nuclear Saturation properties and shell structure

A saturated nuclear density ?

- Liquid-drop model dating back to 1929
- Saturated nuclear matter
- First evidence for a bubble in ^{34}Si
- Renewed interest in nuclear radii: large charge radii
- Shell structure <-> radii and bubbles


ARTICLES
PUBLISHED ONLINE: 24 OCTOBER 2016 | DOI: 10.1038/NPHYS3916
nature physics

A proton density bubble in the doubly magic ^{34}Si nucleus

A. Mutschler[1,2], A. Lemasson[2,3], O. Sorlin[2*], D. Bazin[4], C. Borcea[5], R. Borcea[5], Z. Dombrádi[6], J.-P. Ebran[7], A. Gade[4], H. Iwasaki[4], E. Khan[1], A. Lepailleur[2], F. Recchia[3], T. Roger[2], F. Rotaru[5], D. Sohler[6], M. Stanoiu[5], S. R. Stroberg[4,8], J. A. Tostevin[9], M. Vandebrouck[1], D. Weisshaar[3] and K. Wimmer[3,10,11]

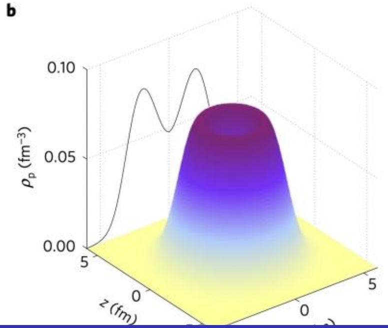

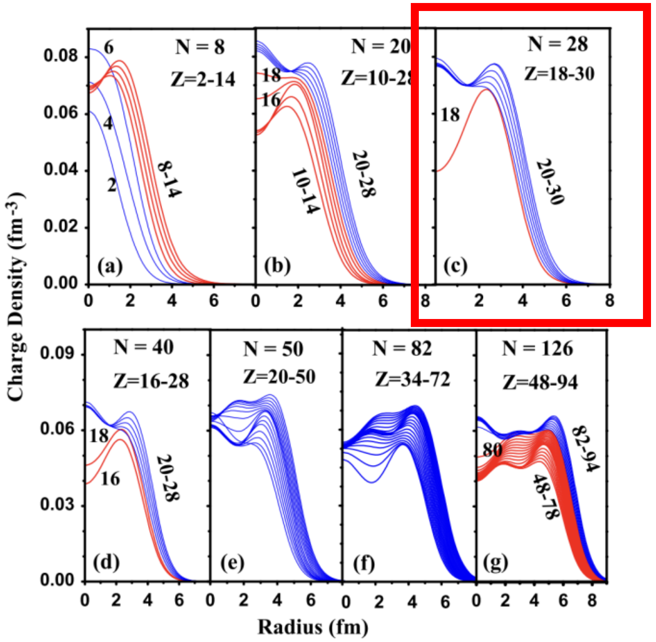

Physics Letters B 788 (2019) 1–6

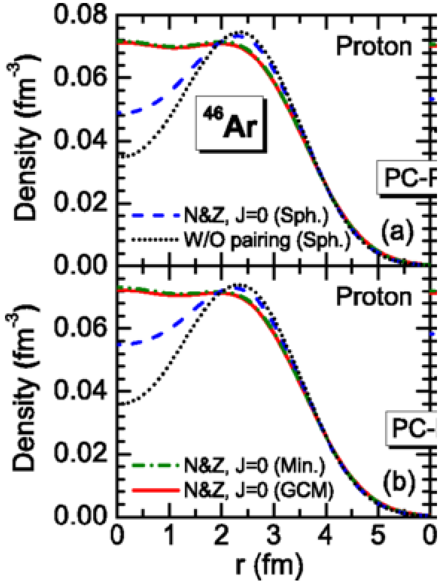

Phys. Rev. C **89**, 017304 (2014)

^{46}Ar: close to stability, but do we understand its structure ?

^{46}Ar: $-2p$ from ^{48}Ca

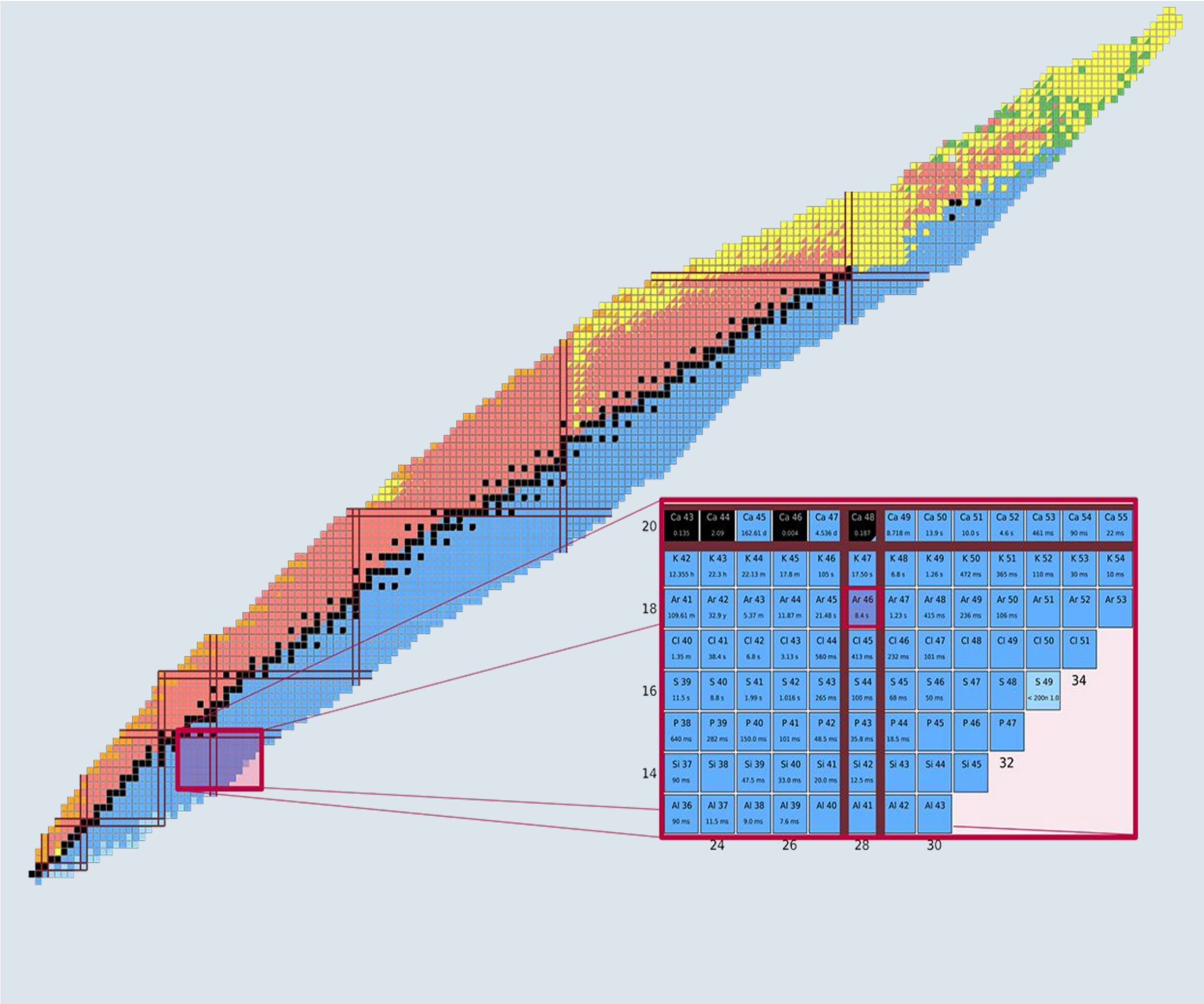

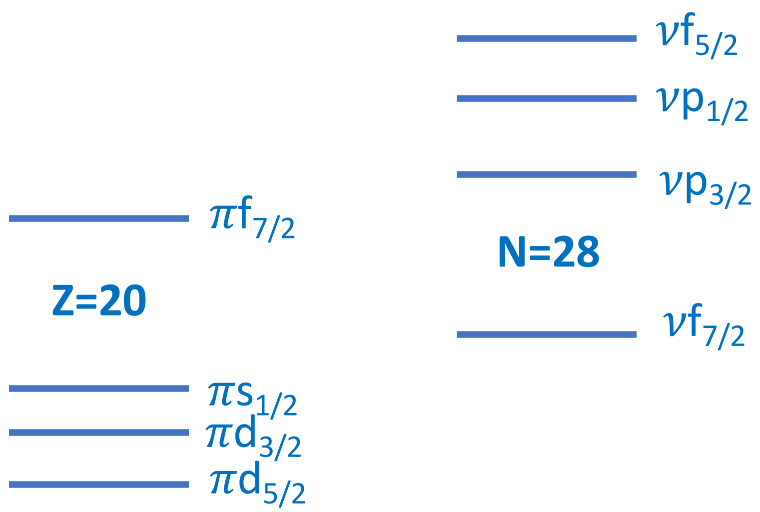

The N=28 shell closure

- The N=28 weakens below ^{48}Ca
- In ^{46}Ar almost one neutron in $p_{3/2}$
- Empirical shell-model Hamiltonians like SDPF-U reproduce the neutron observables very well

Do we understand physics at N=28, Z=18 ?

Neutron observables understood

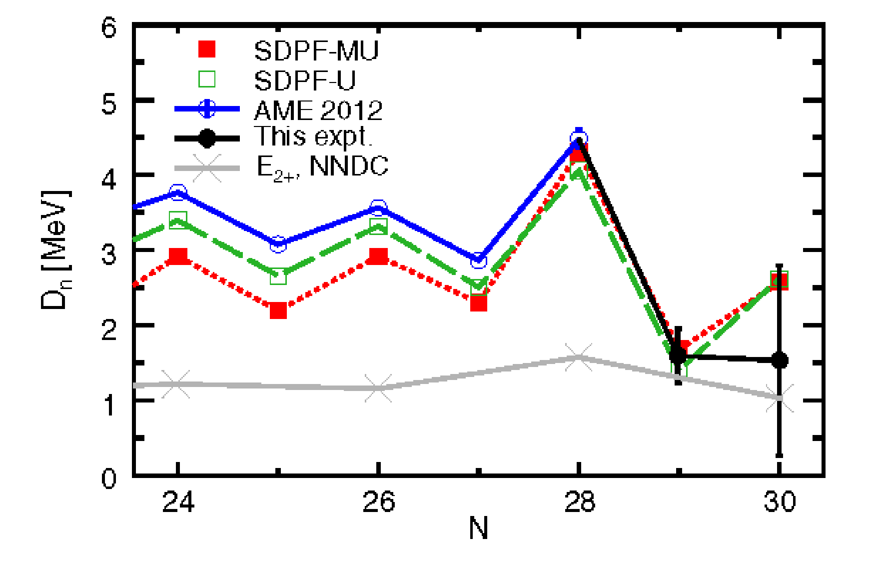

Excellent theory for neutron-space related quantities:

- confirming N=28 shell closure in ^{46}Ar
- SDPF interaction describes valance-core neutrons interaction very well

Z. Meisel et al. PRL 114, 022501 (2015)

Large discrepancy in B(E2)

Large discrepancy with the measured B(E2) value at N=28:

problem with the proton E2 contribution ?

A. Gade et al., PRC 68, 014302 (2003)

S. Calinescu et al., PRC 93, 044333 (2016)

Do we understand physics at N=28 ?

Neutron observables understood

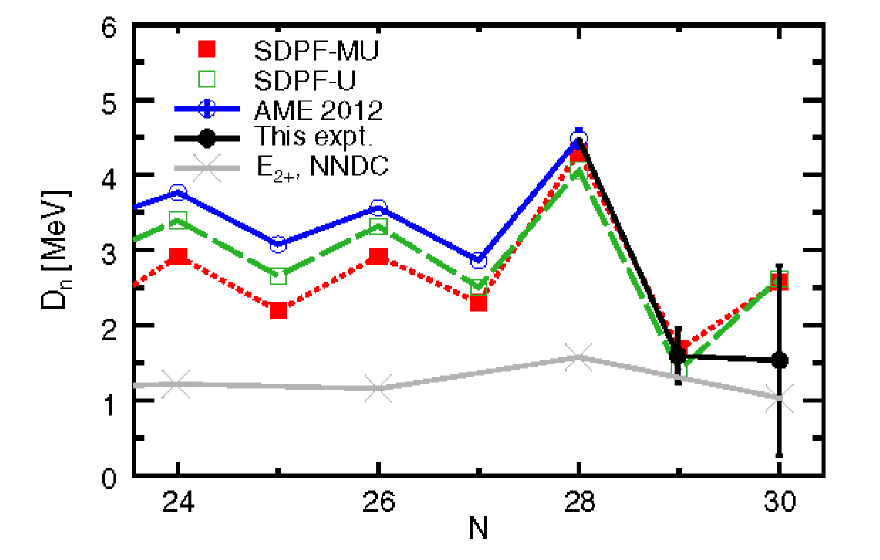

Excellent theory for neutron-space related quantities:

- confirming N=28 shell closure in ^{46}Ar
- SDPF interaction describes valance-core neutrons interaction very well

Z. Meisel et al. PRL 114, 022501 (2015)

Large discrepancy in B(E2)

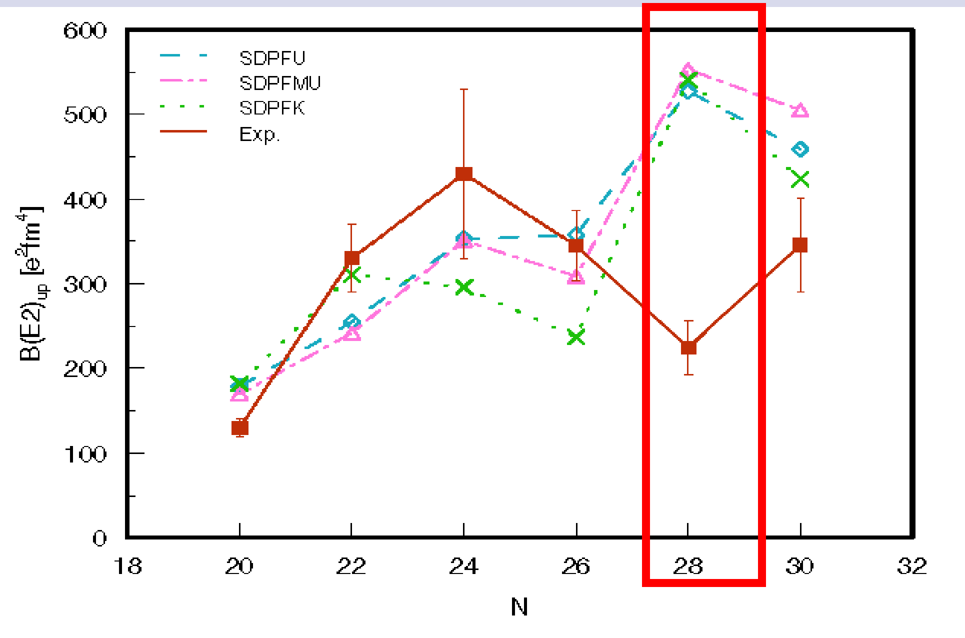

Large discrepancy with the measured B(E2) value at N=28:

problem with the proton E2 contribution ?

A. Gade et al., PRC 68, 014302 (2003)

S. Calinescu et al., PRC 93, 044333 (2016)

Problem with the predicted proton wave function (?)

A. Gade et al., PRC 68, 014302 (2003)

S. Calinescu et al., PRC 93, 044333 (2016)

L. A. Riley et al., PRC 72, 024311 (2005)

- Similar discrepancy in ^{44}S, located −2p with respect to ^{46}Ar
- Intermediate-energy Coulomb excitation measurements in agreement with the SDPF-U results up to ^{42}S
- Effect of polarization charges on B(E 2) calculations is found not sufficient to justify the discrepancy in ^{46}Ar and ^{44}S

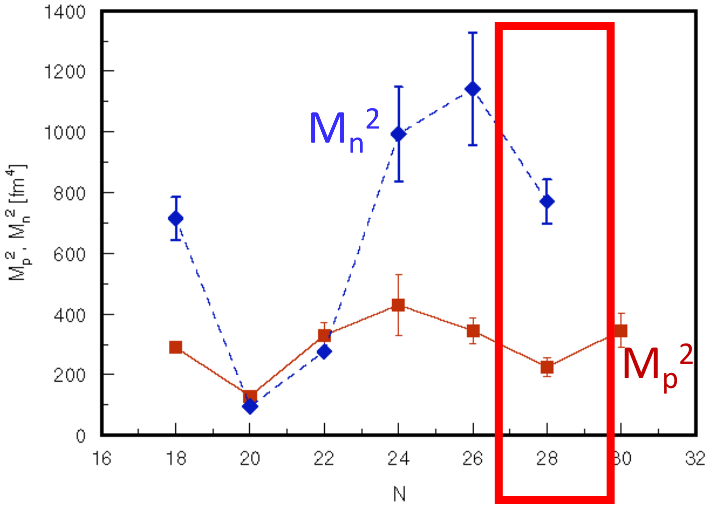

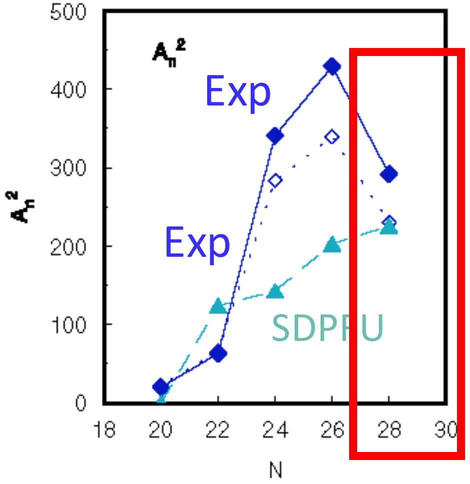

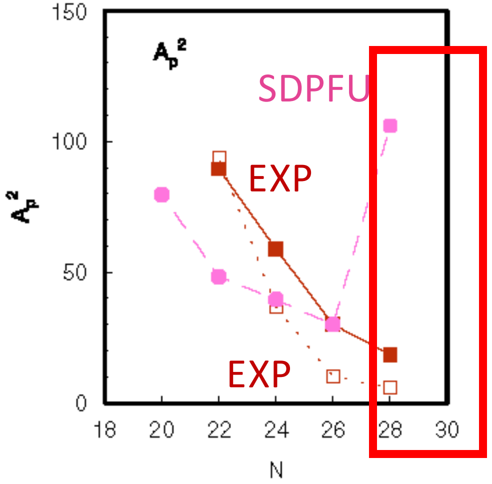

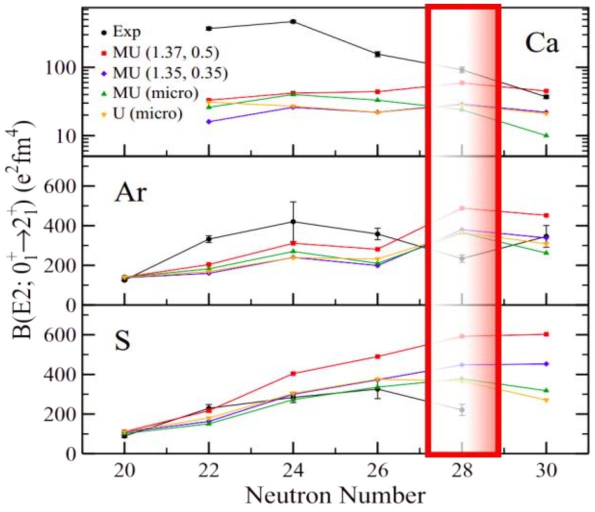

B. Longfellow et al., PRC 103, 054309 (2021)

Need to probe the proton wave function predicted by SDPF:

Example: $\pi s_{1/2}$ almost full or empty in ^{46}Ar to decrease B(E2) to exp. value

Smaller effect from N=28 quenching:with $\nu p_{3/2}$ almost full, B(E2)$_{up}$ in ^{46}Ar still ~ 350 e^{2}fm^4

Direct proton transfer in inverse kinematics

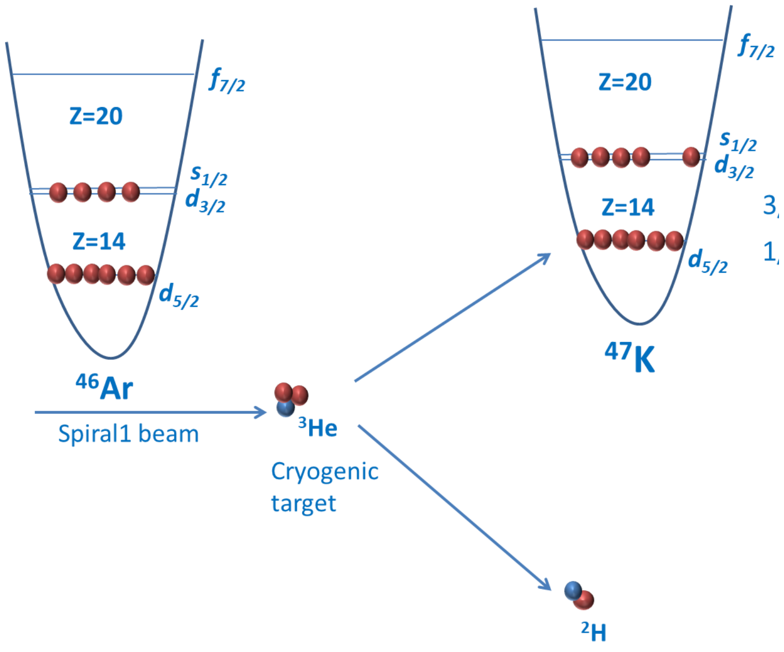

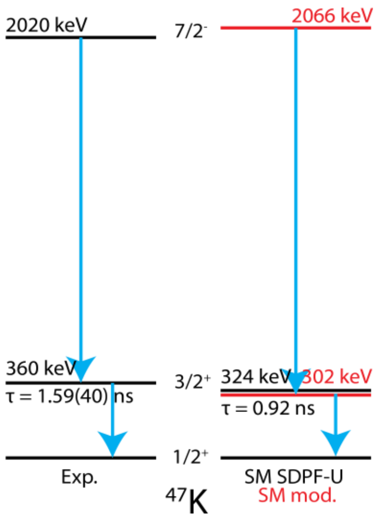

Direct proton-adding reaction to probe the ^{46}Ar ground state wave function

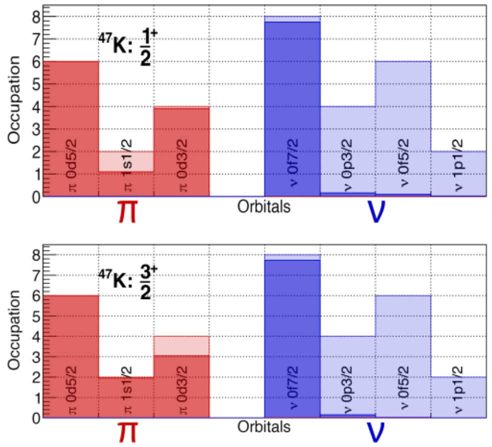

[Banks, S. et al., Nucl. Phys. A 437 2 (1985)]

d laboratory angular distribution

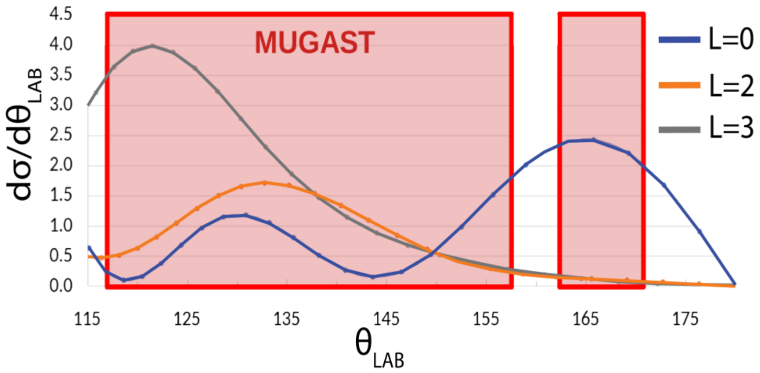

High sensitivity to the transferred wave's L

^{46}Ar predicted wave function

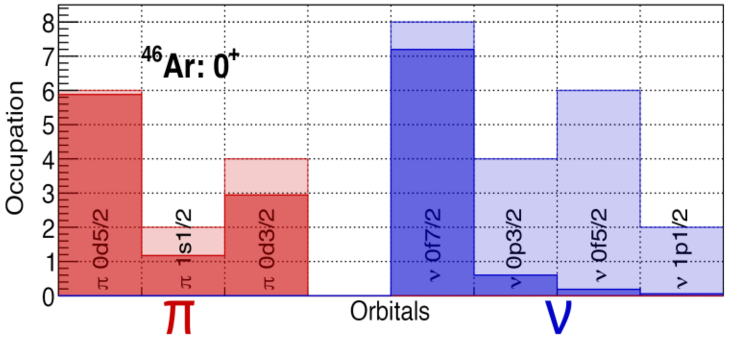

Direct proton transfer in inverse kinematics
@ **GANIL Spiral 1**

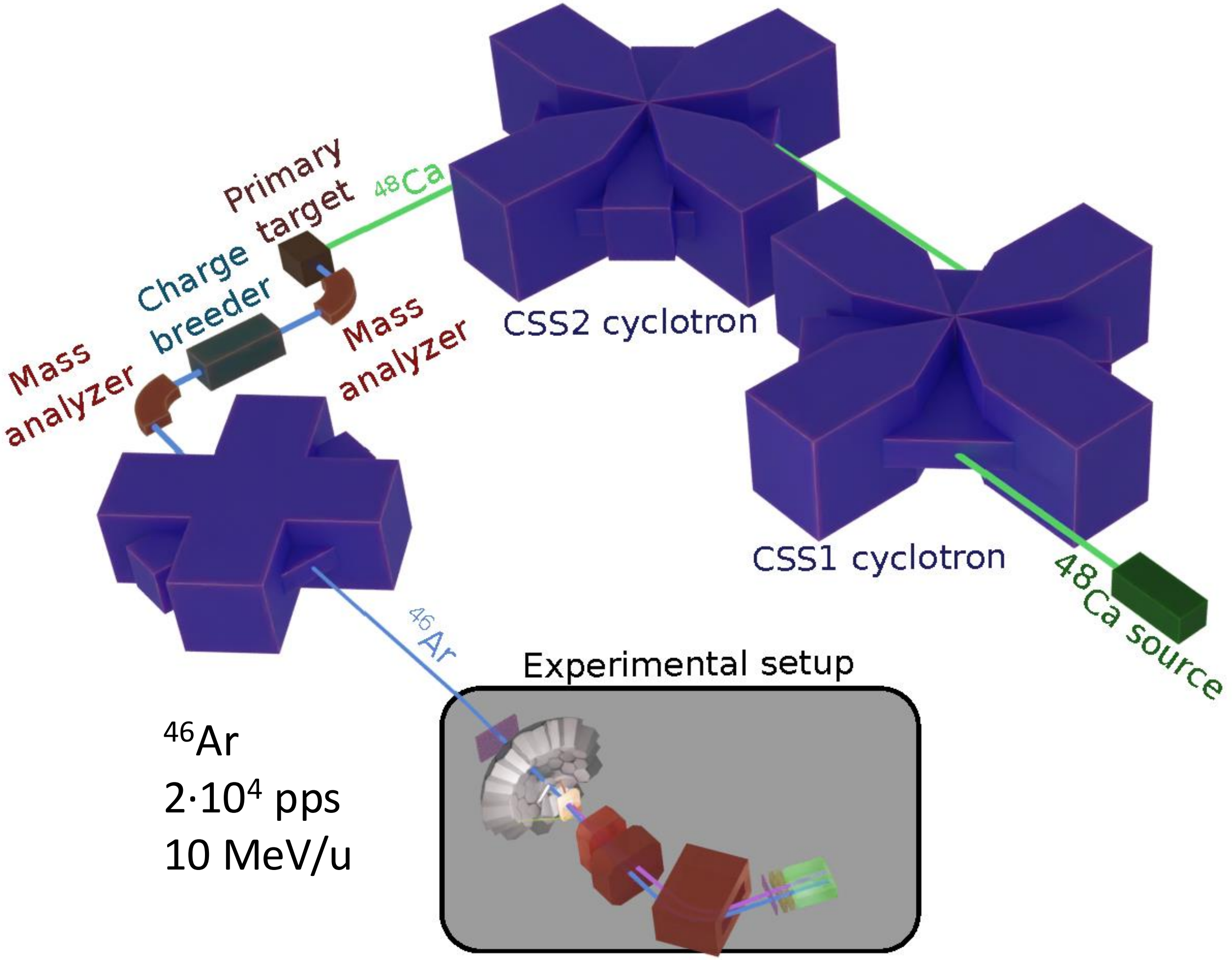

^{48}Ca
60 MeV/u
300-600 W

^{46}Ar
$2 \cdot 10^4$ pps
10 MeV/u

AGATA-MUGAST-VAMOS-HeCTOR

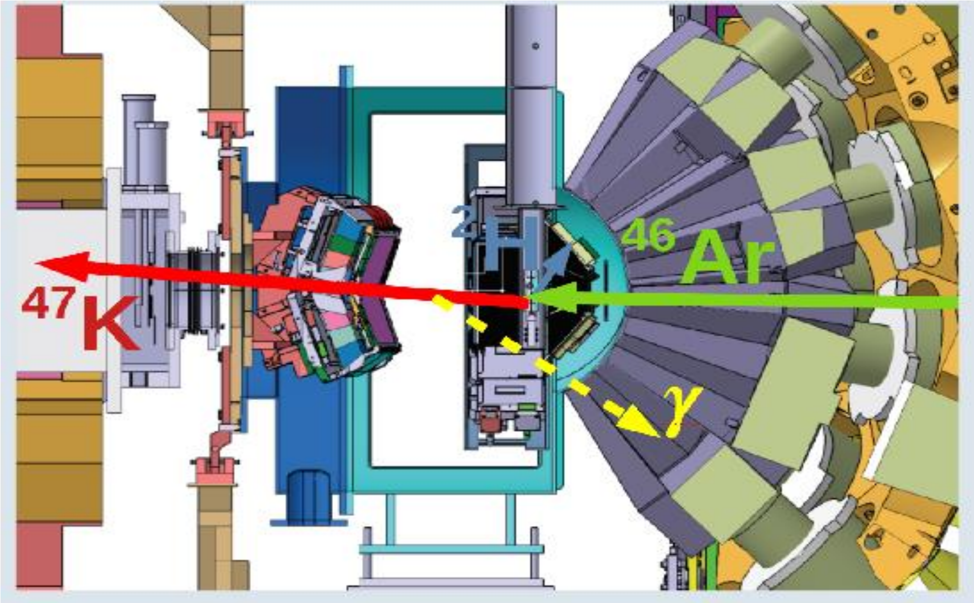

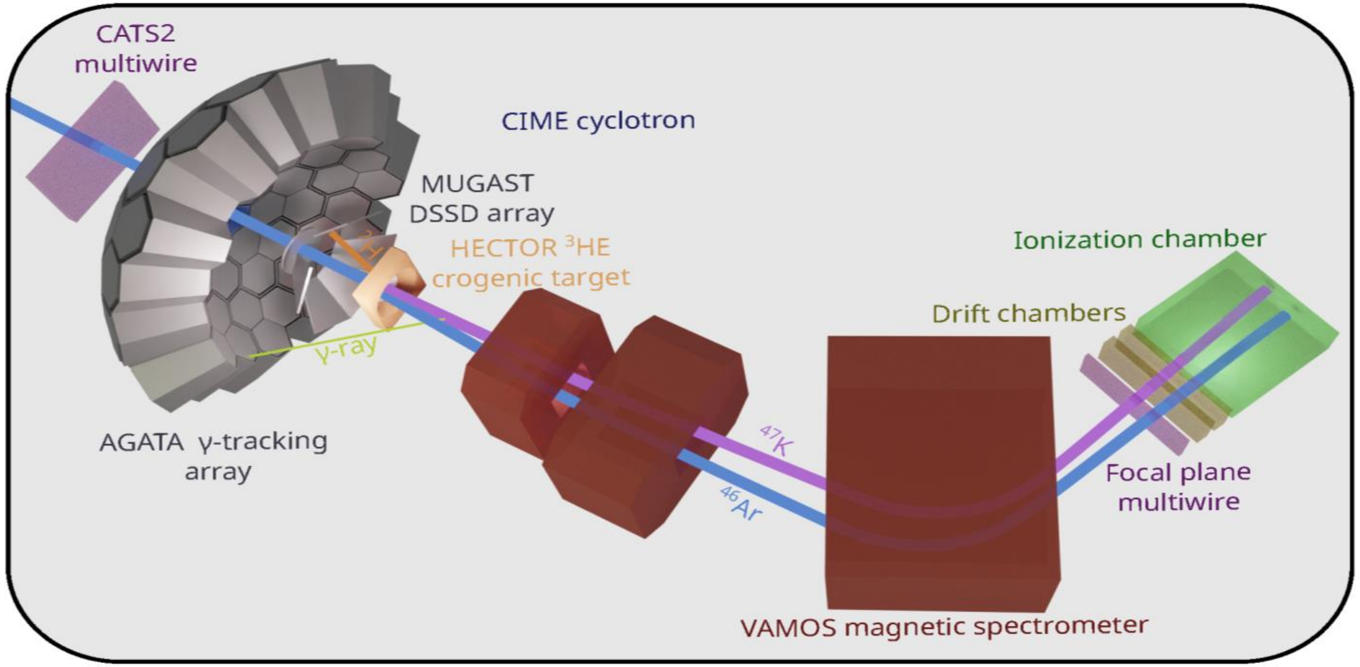

[1] F.Galtarossa et al., NIM A 165830 (2021)

Setup for a complete measurement of reaction-related observables

- HeCTOr: Cryogenic (6 K) ^{3}He target, 3 mm thick – 1 mg/cm^2
- AGATA: γ-ray tracking array, 40 crystals, 10% efficiency
- MUGAST: array of high-granularity DSSD detectors for light ejectiles
- VAMOS: mass spectrometer
- CATS2: beam tracking gas detectors

AGATA - VAMOS

Mass and Z identification in VAMOS

- Z identification through IC

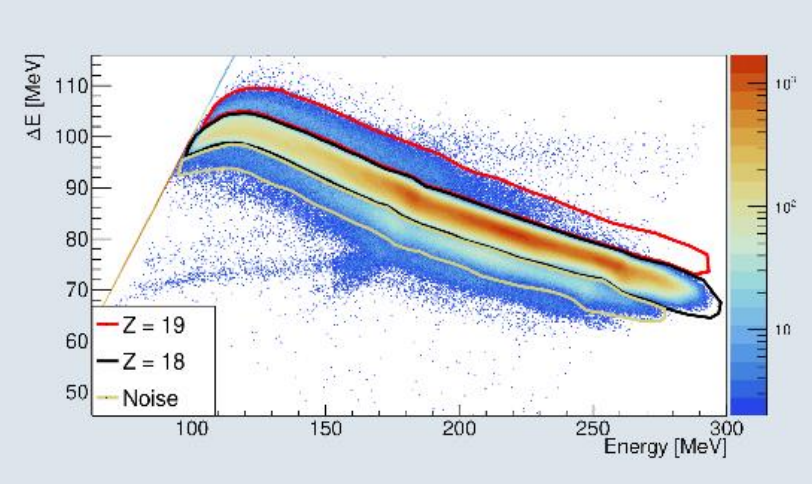

- Mass identification
- Beam monitoring

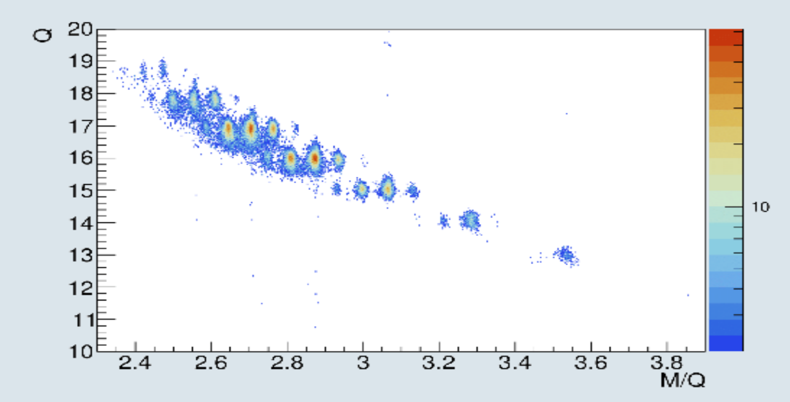

γ-ray spectra from AGATA

- Doppler corrected γ-ray spectra in coincidence with ^{47}K in VAMOS
- Compared with Geant4 simulations of the AGATA response function for different level (lifetime) population. HeCTOr geometry taken into account

AGATA - VAMOS

Mass and Z identification in VAMOS

- Z identification through IC

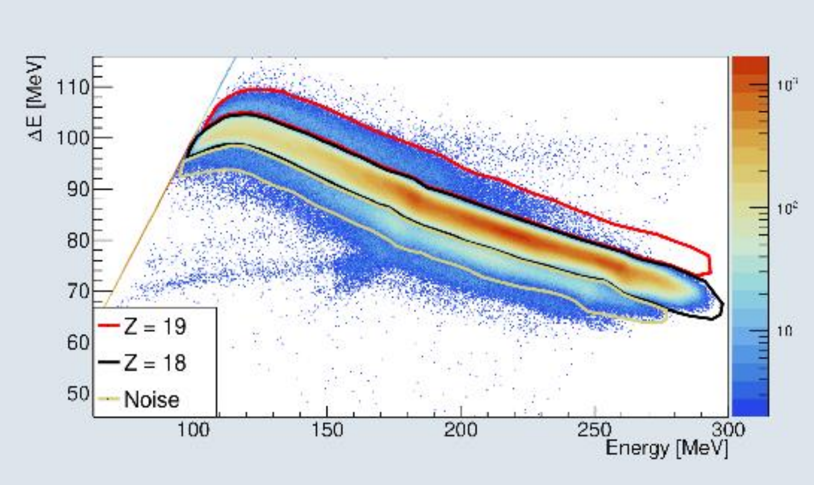

- Mass identification
- Beam monitoring

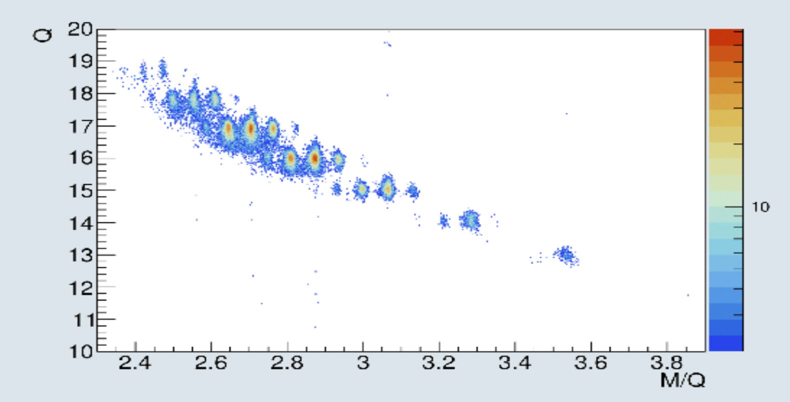

γ-ray spectra from AGATA

- Doppler corrected γ-ray spectra in coincidence with ^{47}K in VAMOS
- Compared with Geant4 simulations of the AGATA response function for different level (lifetime) population. HeCTOr geometry taken into account

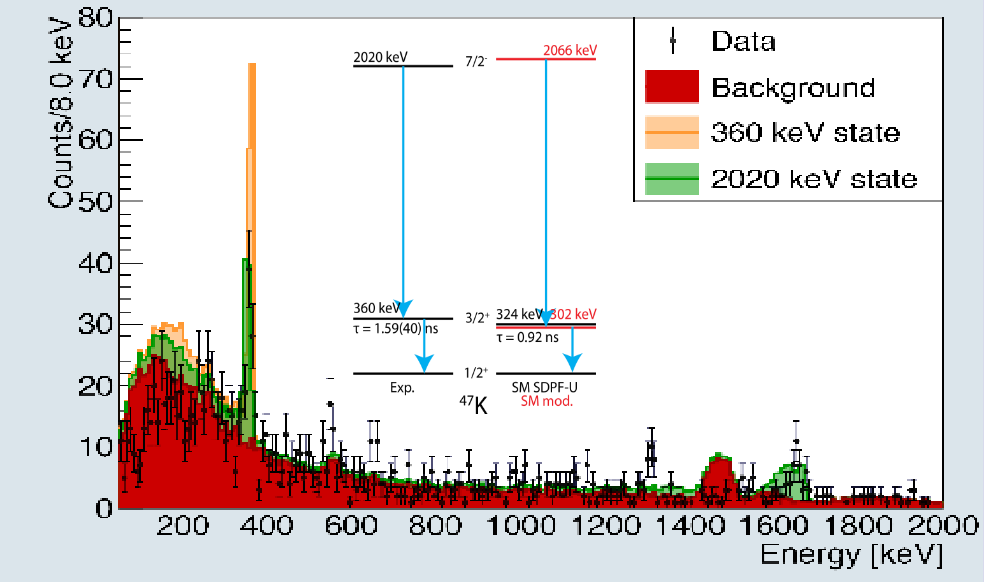

HeCTOr, MUGAST (towards GRIT)

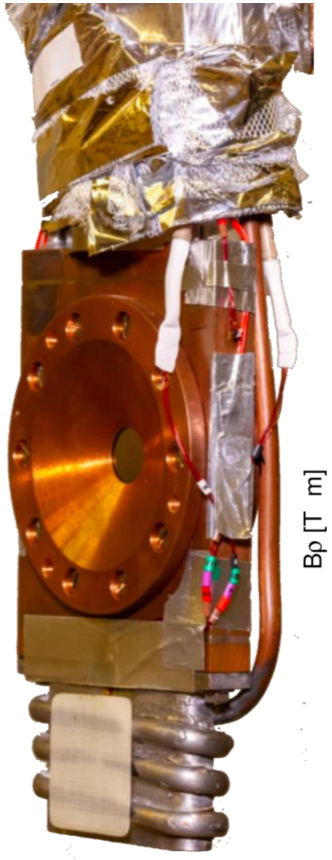

- 3 mm nominal thickness
- $T \approx 6$K, $P \leq 1$ bar $\Rightarrow 1.2$ mg/cm^2
- Havar windows of 3.8 μm thickness
- 16 mm diameter
- Angles close to 90° are not accessible, no elastic scattering measurements

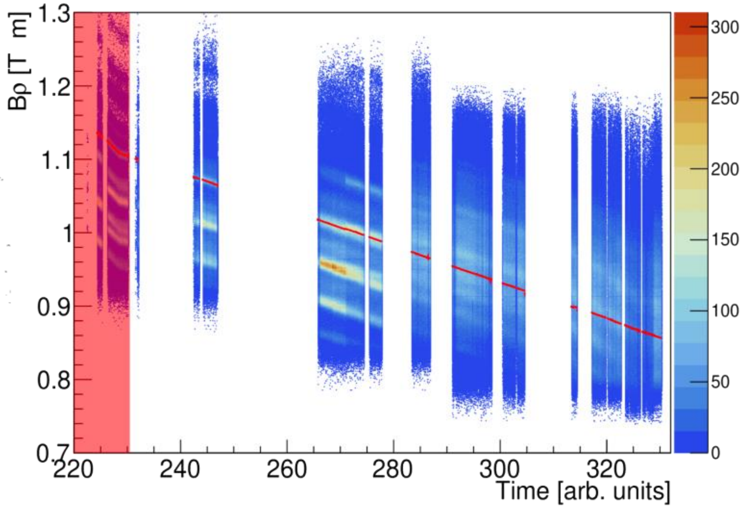

Ice deposition over time monitored with VAMOS

MUGAST [M. Assié et al., NIM A 1014, 165743 (2021)]

- First step of the GRIT project (together with Must2)
- 5 trapezoidal detectors, 1 annular detector placed at backwards angles
- Each trapezoid is segmented for position resolution with 128 X-strips and 128 Y-strips
- Particle discrimination with E-TOF using Cats2, a position-sensitive beam tracker

Geant4 Monte-Carlo simulation returns efficiency performance of the array

HeCTOr, MUGAST (towards GRIT)

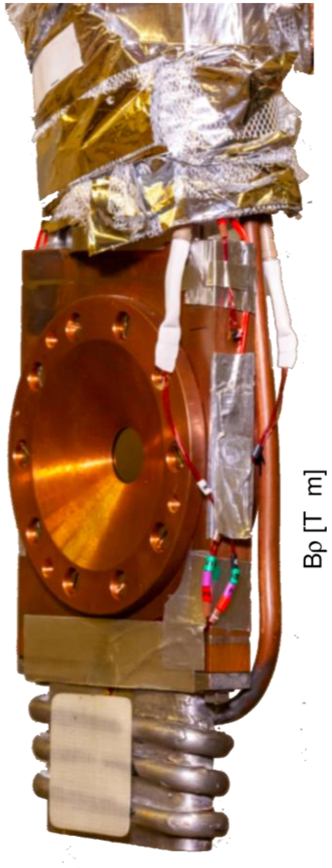

- 3 mm nominal thickness
- $T \approx 6$K, $P \lesssim 1$ bar $= \Rightarrow 1.2$ mg/cm^2
- Havar windows of 3.8 μm thickness
- 16 mm diameter
- Angles close to 90° are not accessible, no elastic scattering measurements

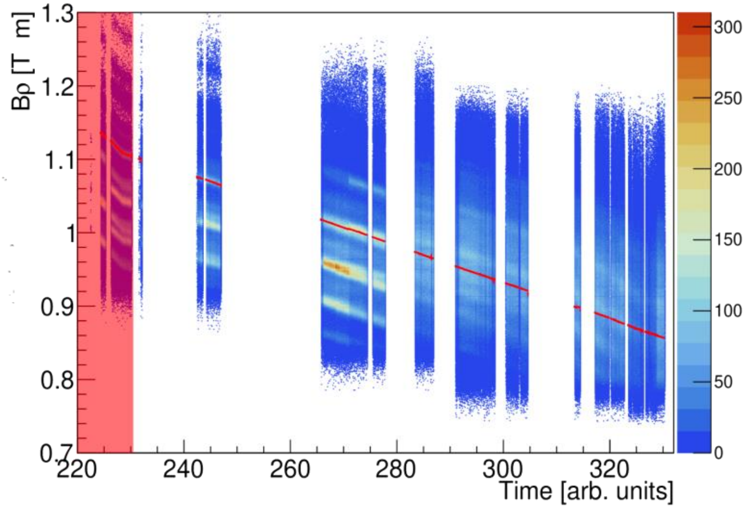

Ice deposition over time monitored with VAMOS

MUGAST [M. Assié et al., NIM A 1014, 165743 (2021)]

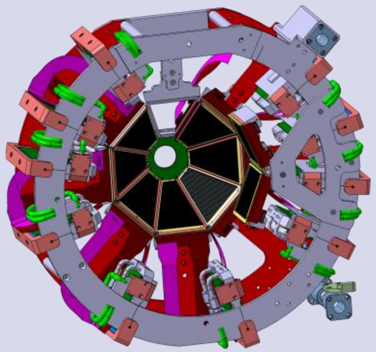

- First step of the GRIT project (together with Must2)
- 5 trapezoidal detectors, 1 annular detector placed at backwards angles
- Each trapezoid is segmented for position resolution with 128 X-strips and 128 Y-strips
- Particle discrimination with E-TOF using Cats2, a position-sensitive beam tracker

Geant4 Monte-Carlo simulation returns efficiency performance of the array

MUGAST-AGATA: particle and γ-ray spectra

Particle spectra from MUGAST-VAMOS coinc.

- Z identification through E-TOF
- Strong ^{46}Ar(^{3}He,pn)^{47}K channel

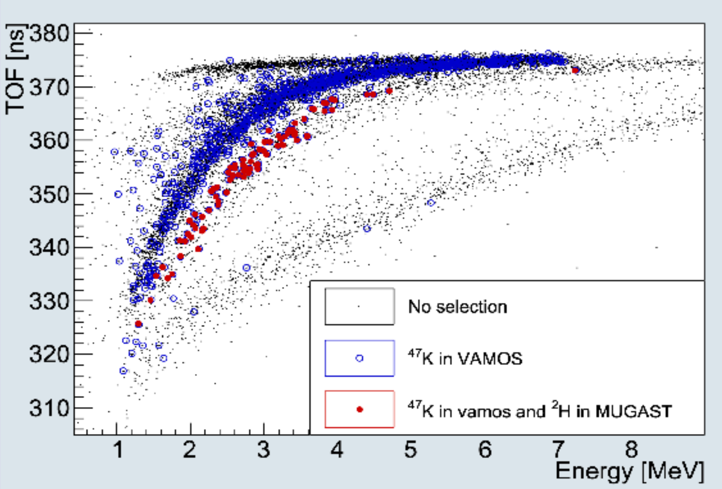

- Excitation energy recalculated with energy loss corr.

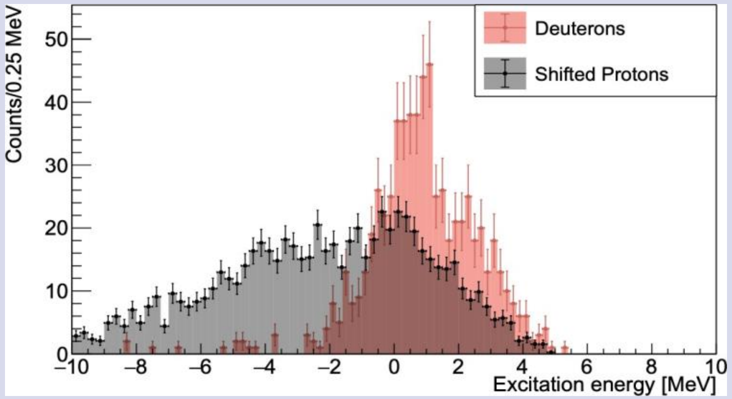

γ-ray spectra from AGATA-MUGAST-VAMOS

- Doppler corrected γ-ray spectra in coincidence with ^{47}K in VAMOS **AND** deuterons in Mugast

MUGAST-AGATA: particle and γ-ray spectra

Particle spectra from MUGAST-VAMOS coinc.

- Z identification through E-TOF
- Strong ^{46}Ar(^{3}He,pn)^{47}K channel

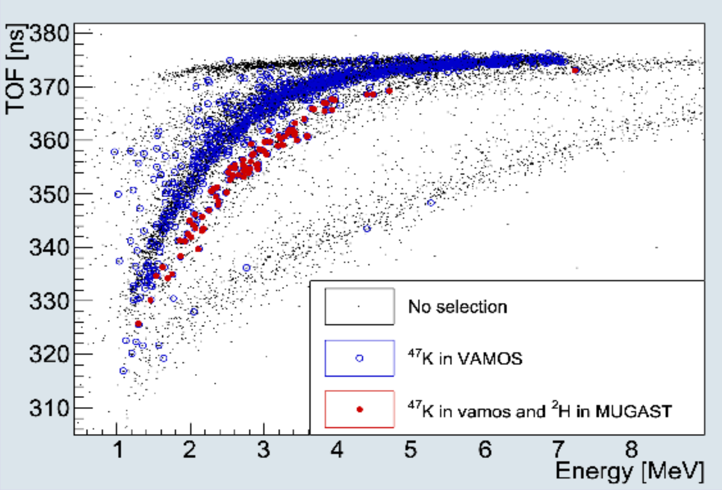

- Excitation energy recalculated with energy loss corr.

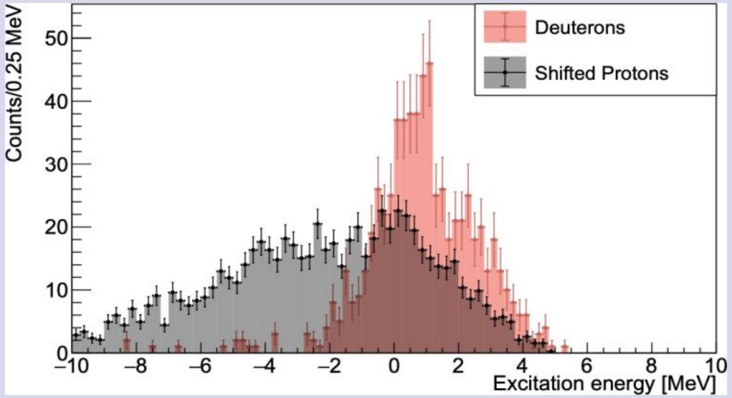

γ-ray spectra from AGATA-MUGAST-VAMOS

- Doppler corrected γ-ray spectra in coincidence with ^{47}K in VAMOS **AND** deuterons in Mugast

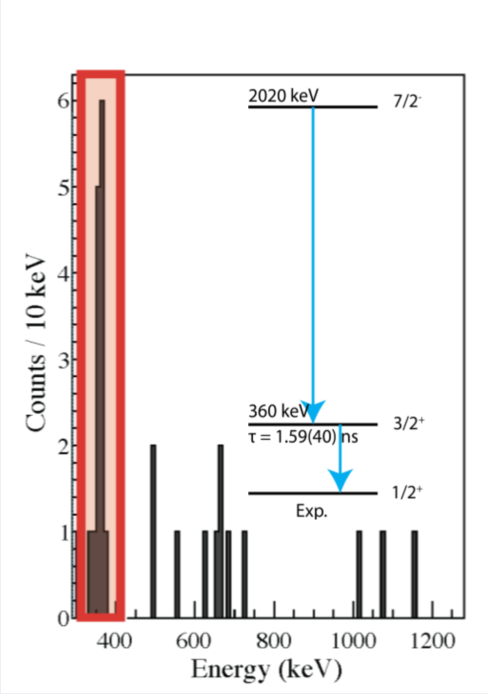

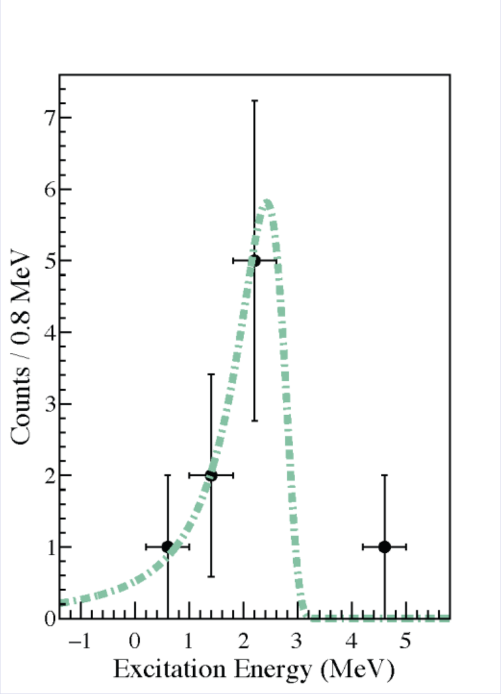

Data analysis: Monte Carlo-simulation based approach

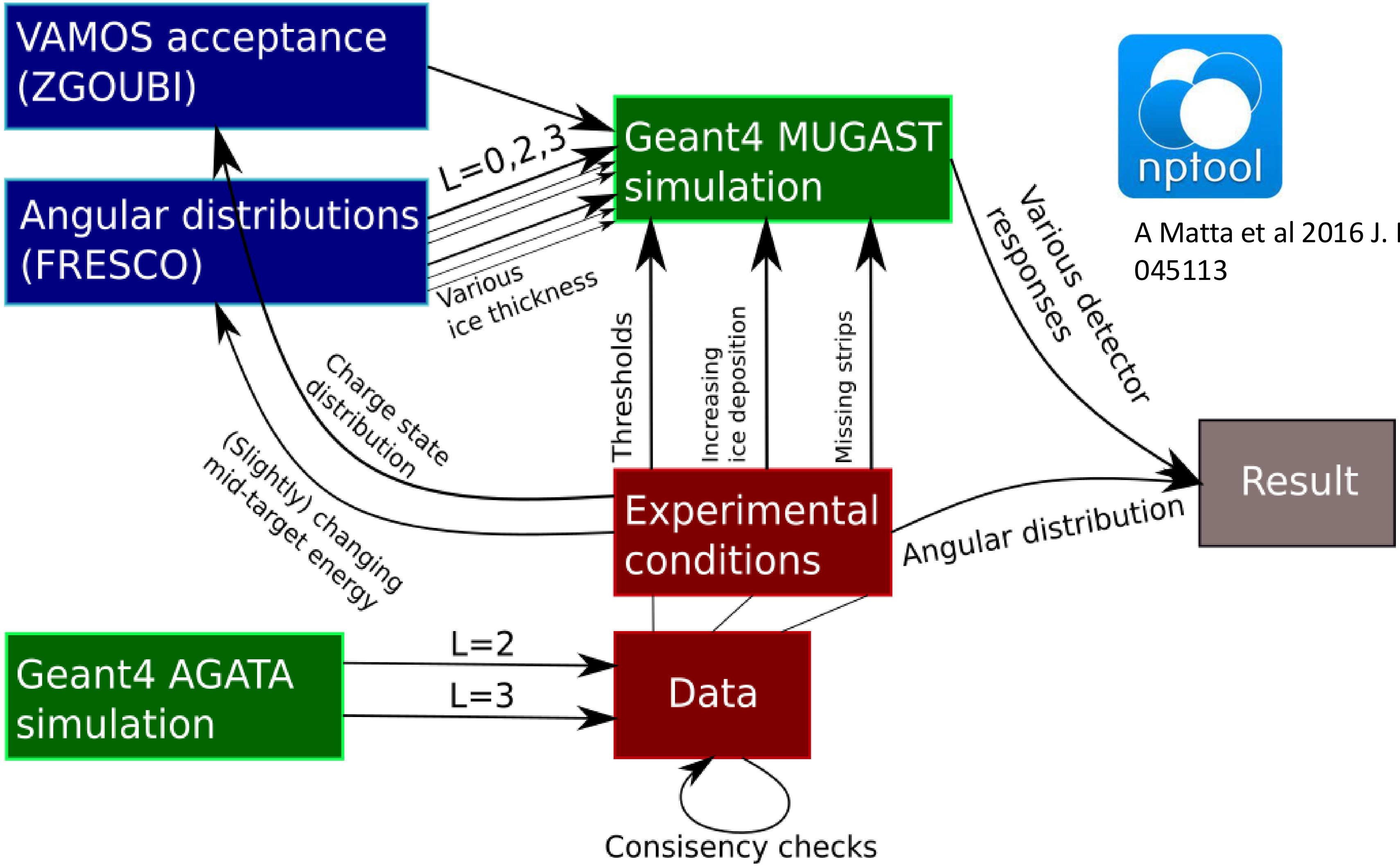

nptool

A Matta et al 2016 J. Phys. G: Nucl. Part. Phys. 43 045113

Data analysis: angular distributions

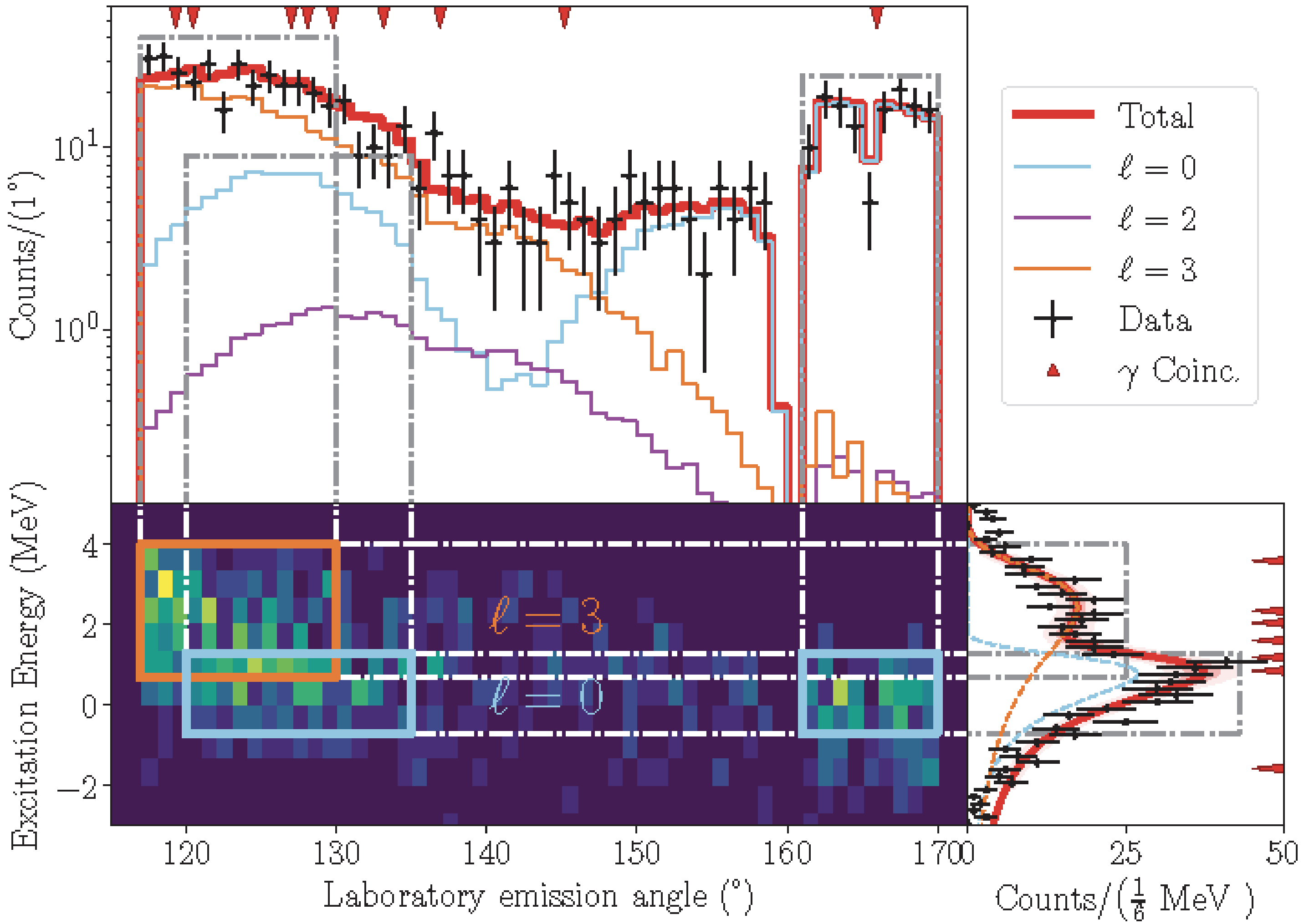

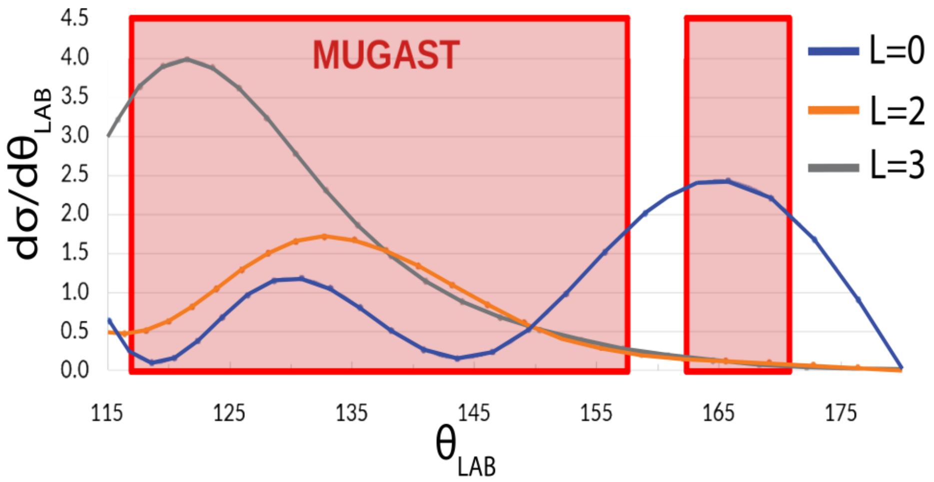

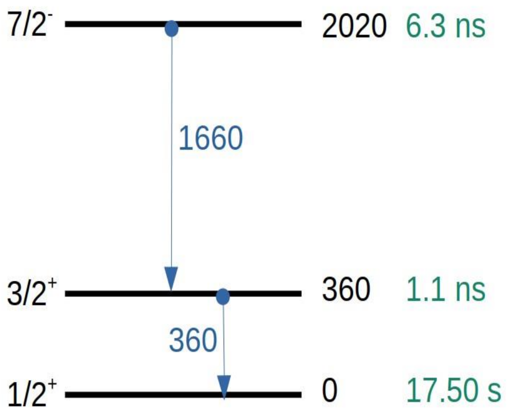

The ^{47}K-*d* optical potential

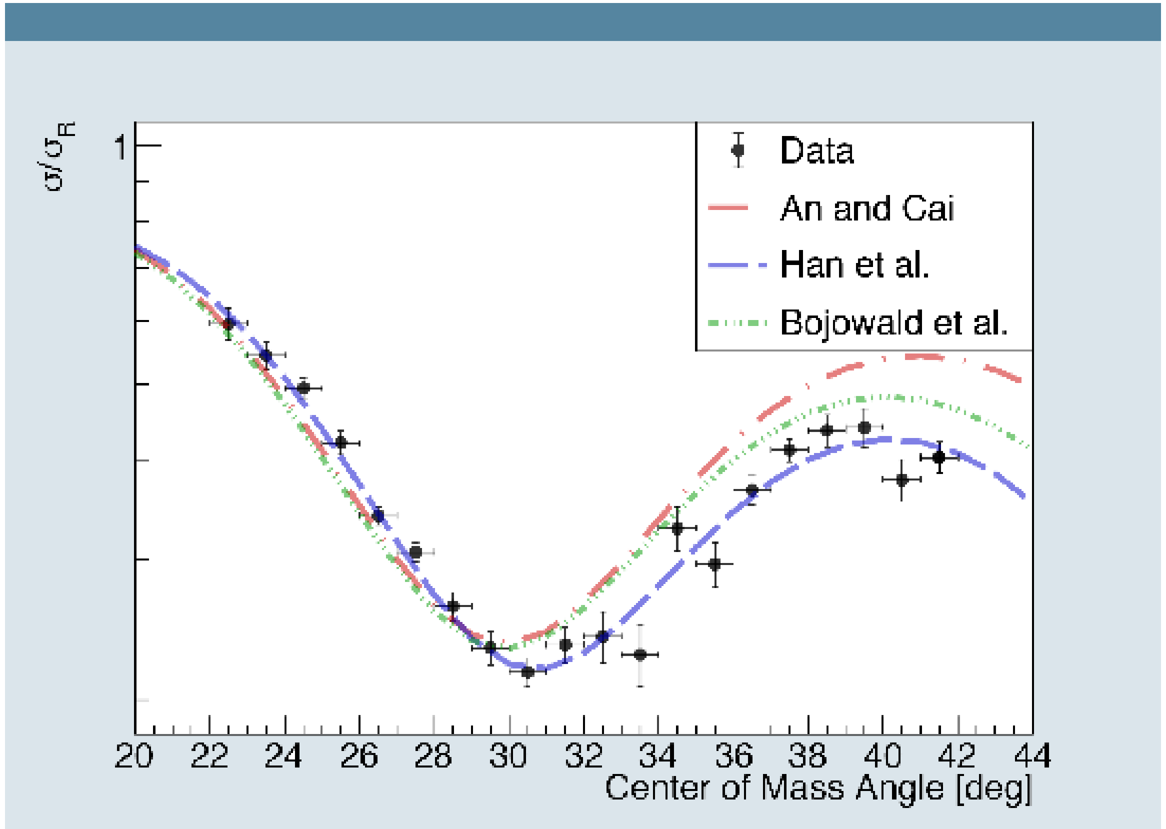

- Elastic scattering of the ^{47}K(d,d)^{47}K reaction at 7.52 MeV/u
  Paxman, C. and the e793s collaboration., Priv. Comm
- The incoming optical potential (^{46}Ar-^{3}He) could not be assessed due to the impossibility of measuring the elastic scattering

The ^{48}Ca(d, ^{3}He)^{47}K direct reaction (I)

Exp. data [Banks, S. et al., Nucl. Phys. A 437 2 (1985)]

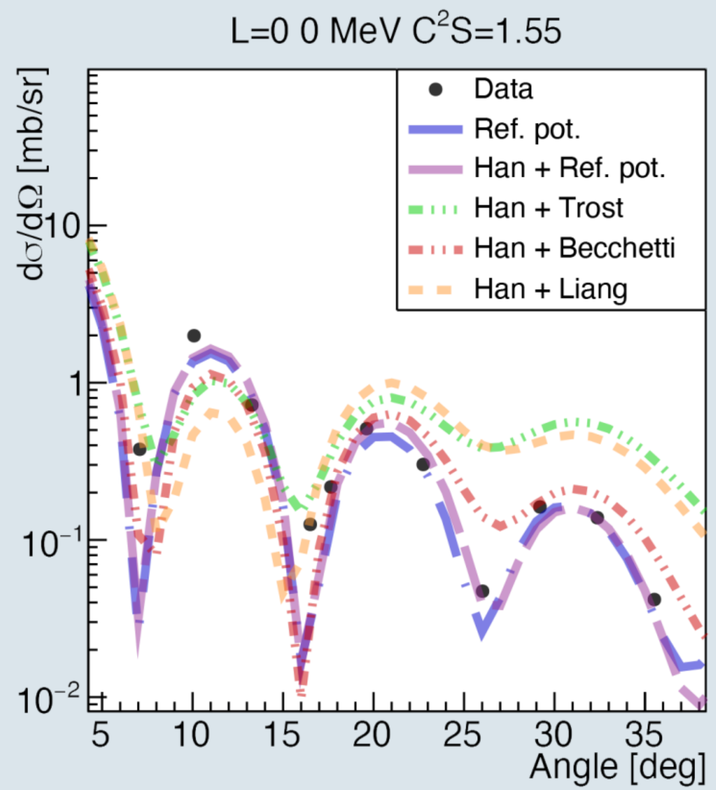

- Finite-range FRESCO calculation
- The $j = 1/2$ and $j = 3/2$ strengths appear with little fragmentation as only two states are observed, exhausting the SP strength in both cases
- The best-performing optical potential is the combination of [Becchetti et al. , Polarization Phenomena in Nuclear Reactions (1971)] for the ^{3}He and [Han et al., PRC 74, 044615 (2006)] for the d

The $^{48}Ca(d, {}^3He)^{47}K$ direct reaction (II)

Exp. data [Banks, S. et al., Nucl. Phys. A 437 2 (1985)]

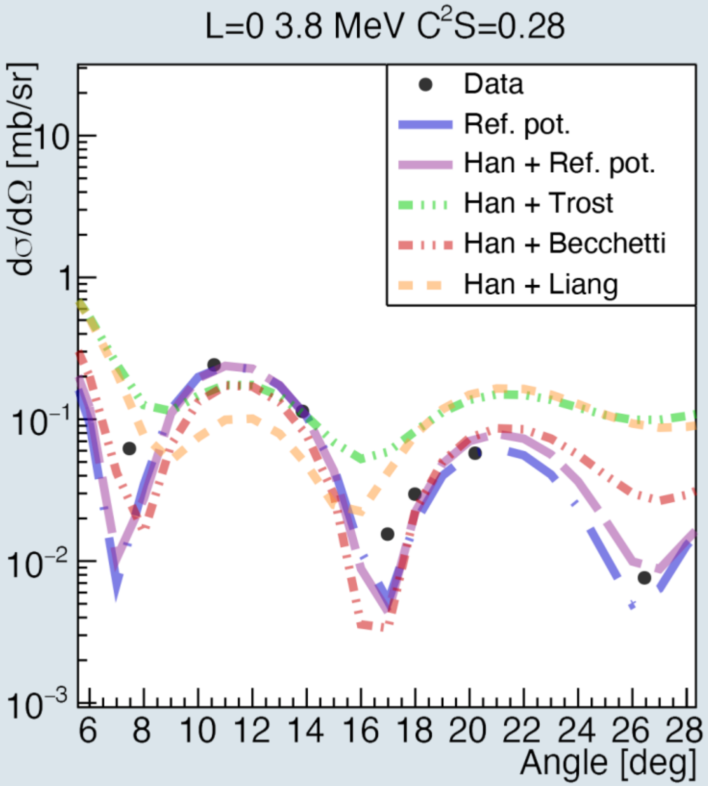

- Finite-range FRESCO calculation
- The $j = 1/2$ and $j = 3/2$ strengths appear with little fragmentation as only two states are observed, exhausting the SP strength in both cases
- The best-performing optical potential is the combination of [Becchetti et al. , Polarization Phenomena in Nuclear Reactions (1971)] for the ^3He and [Han et al., PRC 74, 044615 (2006)] for the d

The ^{48}Ca(d, ^{3}He)^{47}K direct reaction (III)

Exp. data [Banks, S. et al., Nucl. Phys. A 437 2 (1985)]

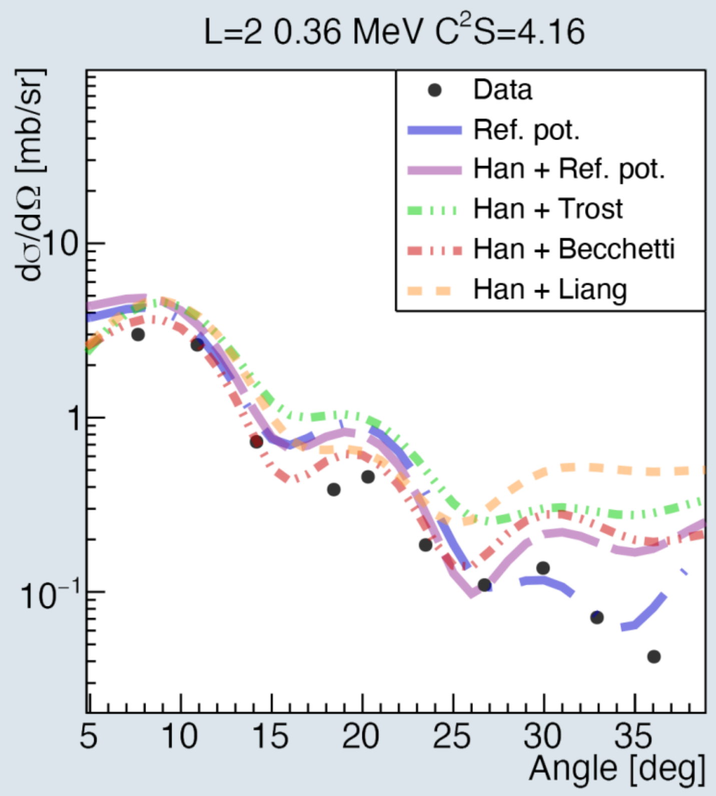

- Finite-range FRESCO calculation
- The j = 1/2 and j = 3/2 strengths appear with little fragmentation as only two states are observed, exhausting the SP strength in both cases
- The best-performing optical potential is the combination of [Becchetti et al. , Polarization Phenomena in Nuclear Reactions (1971)] for the ^{3}He and [Han et al., PRC 74, 044615 (2006)] for the d

The ^{48}Ca(d, ^{3}He)^{47}K direct reaction (IV)

Exp. data [Banks, S. et al., Nucl. Phys. A 437 2 (1985)]

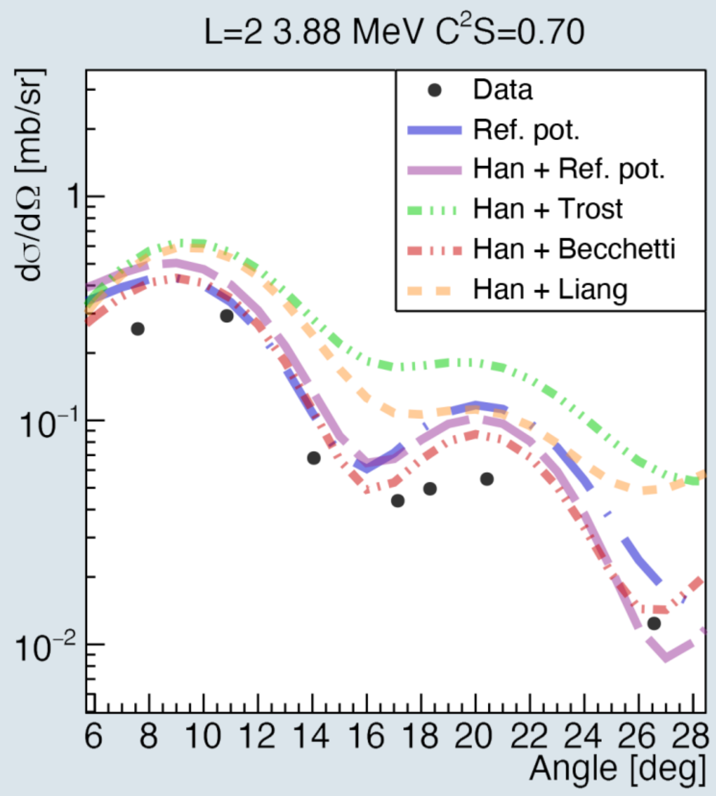

- Finite-range FRESCO calculation
- The j = 1/2 and j = 3/2 strengths appear with little fragmentation as only two states are observed, exhausting the SP strength in both cases
- The best-performing optical potential is the combination of [Becchetti et al. , Polarization Phenomena in Nuclear Reactions (1971)] for the ^{3}He and [Han et al., PRC 74, 044615 (2006)] for the d

The ^{46}Ar(^{3}He, d)^{47}K direct reaction (I)

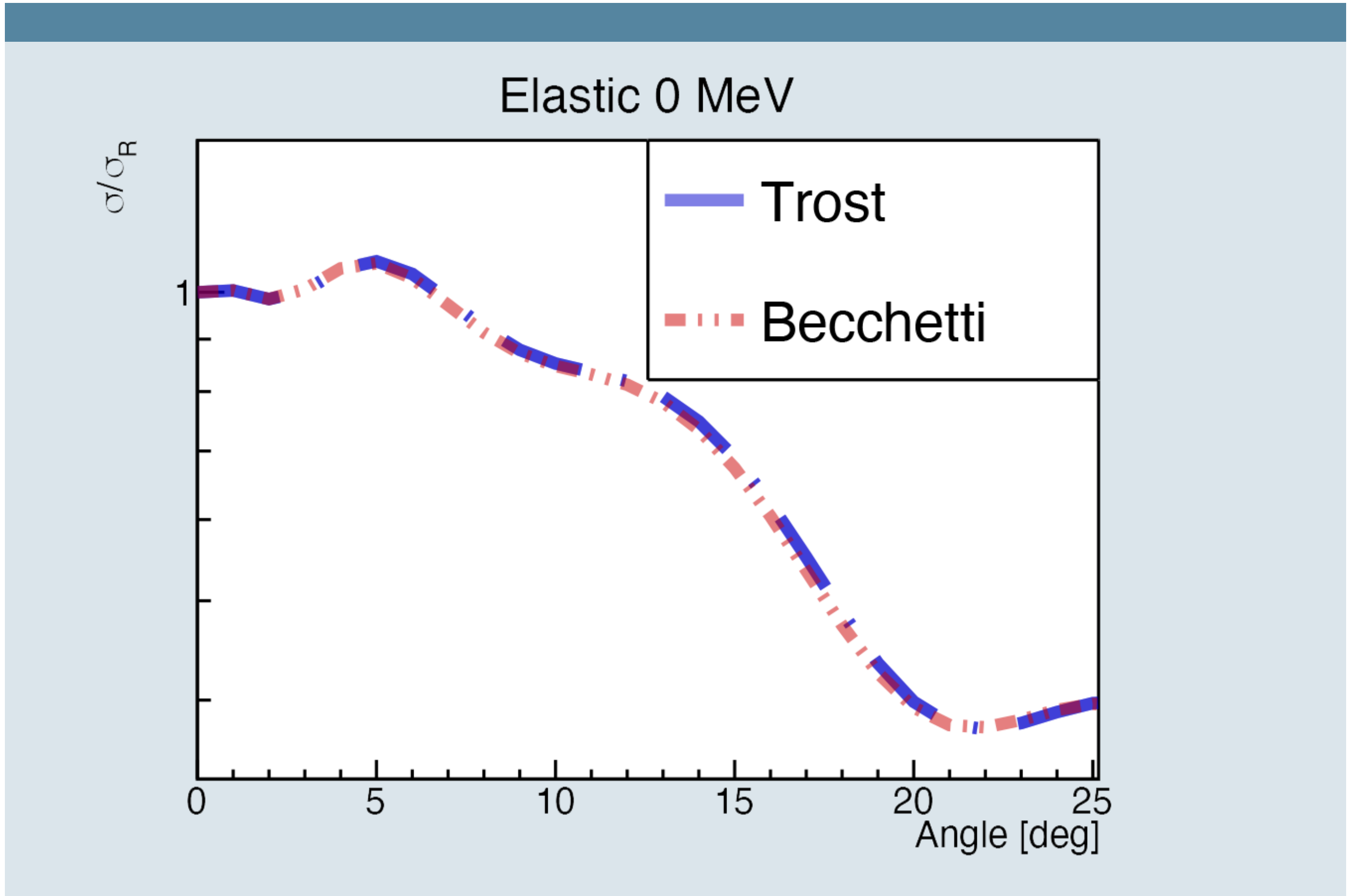

- Finite-range FRESCO calculation
- The position of the maxima of the distributions is affected minimally by the optical potential choice
- These calculations will serve as an input for the Geant4 Monte Carlo simulations

The ^{46}Ar(^{3}He, *d*)^{47}K direct reaction (II)

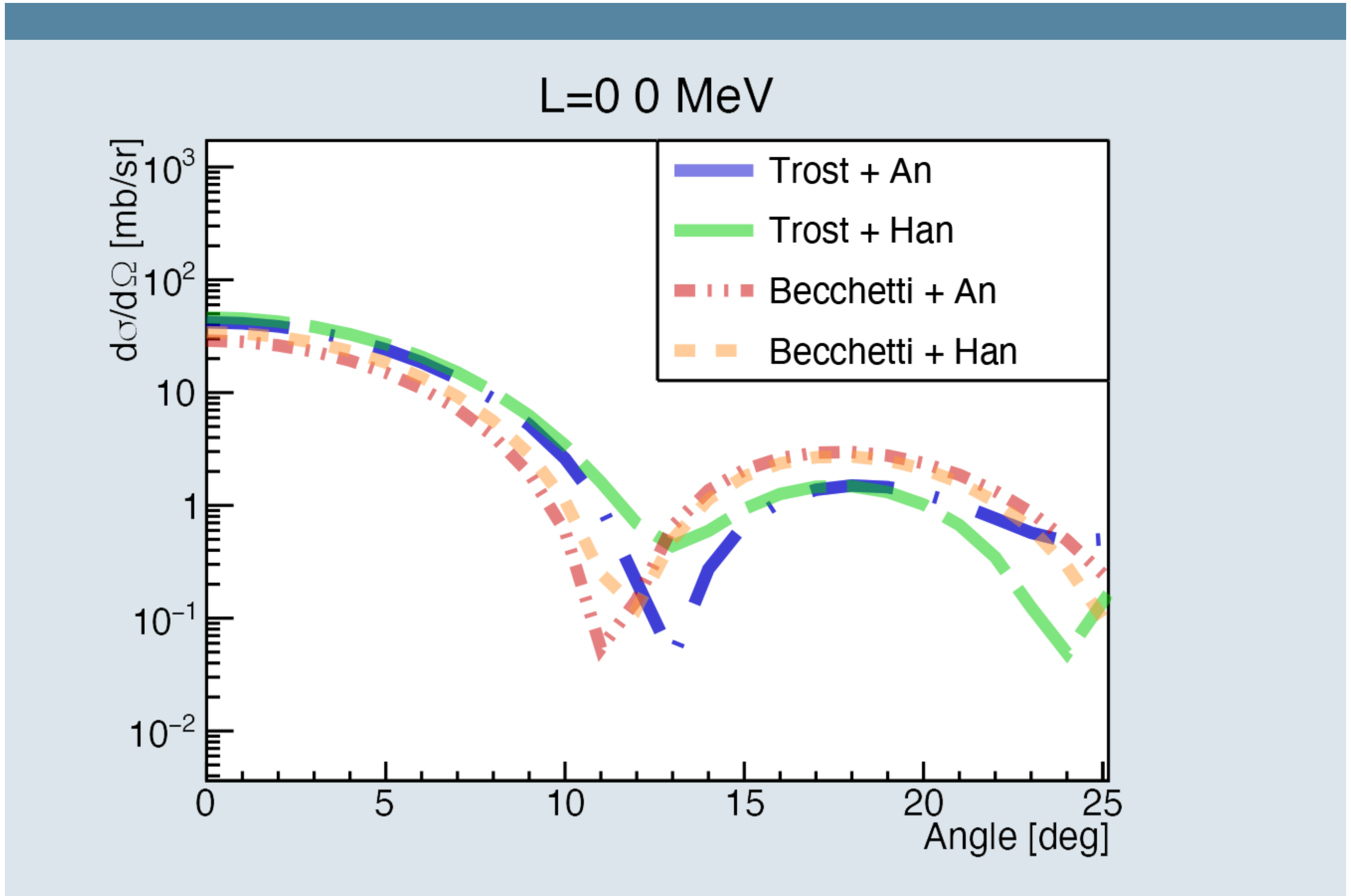

- Finite-range FRESCO calculation
- The position of the maxima of the distributions is affected minimally by the optical potential choice
- These calculations will serve as an input for the Geant4 Monte Carlo simulations

The ^{46}Ar(^{3}He, *d*)^{47}K direct reaction (III)

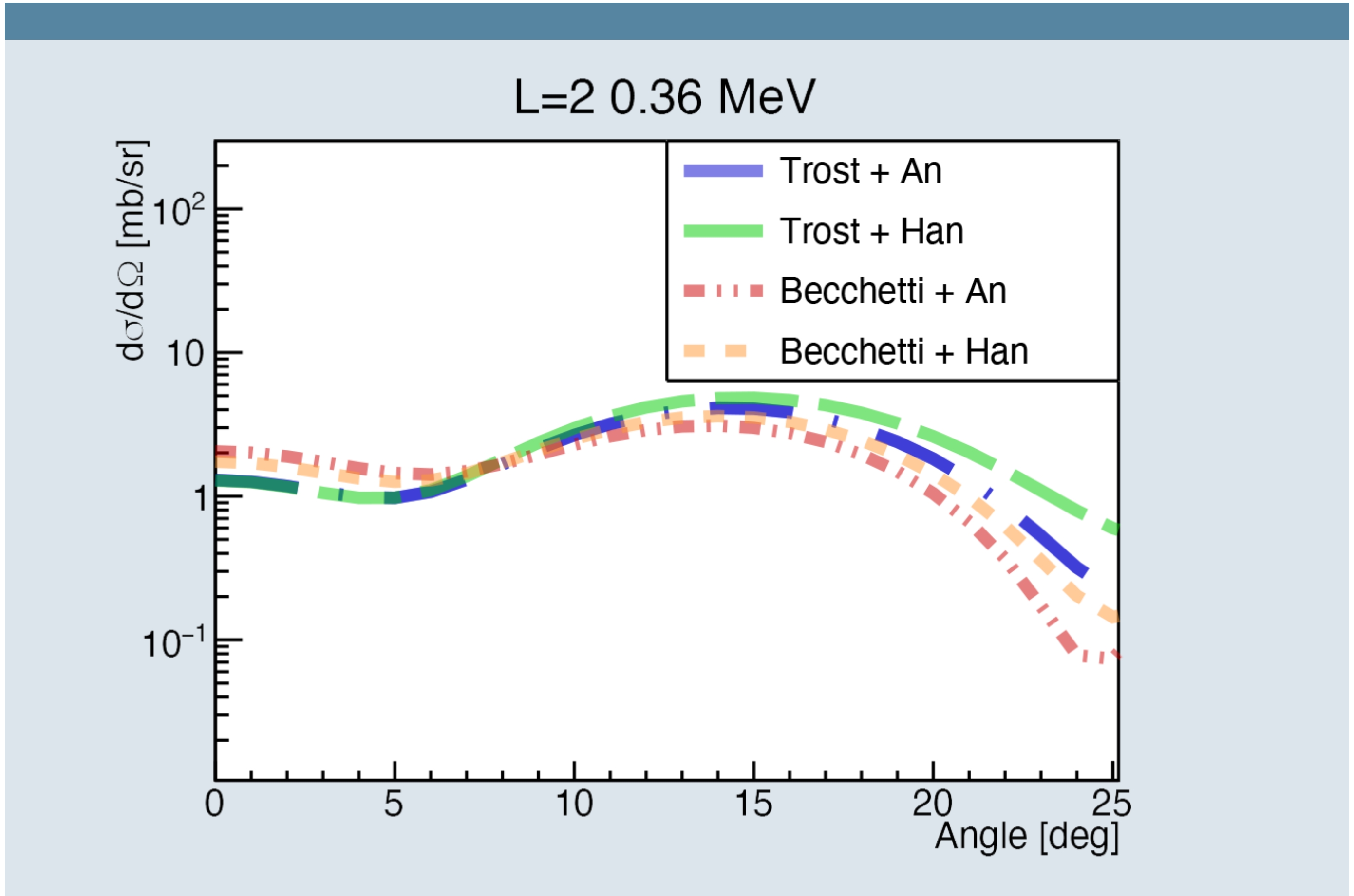

- Finite-range FRESCO calculation
- The position of the maxima of the distributions is affected minimally by the optical potential choice
- These calculations will are an input for the Geant4 Monte Carlo simulations

The ^{46}Ar(^{3}He, d)^{47}K direct reaction (IV)

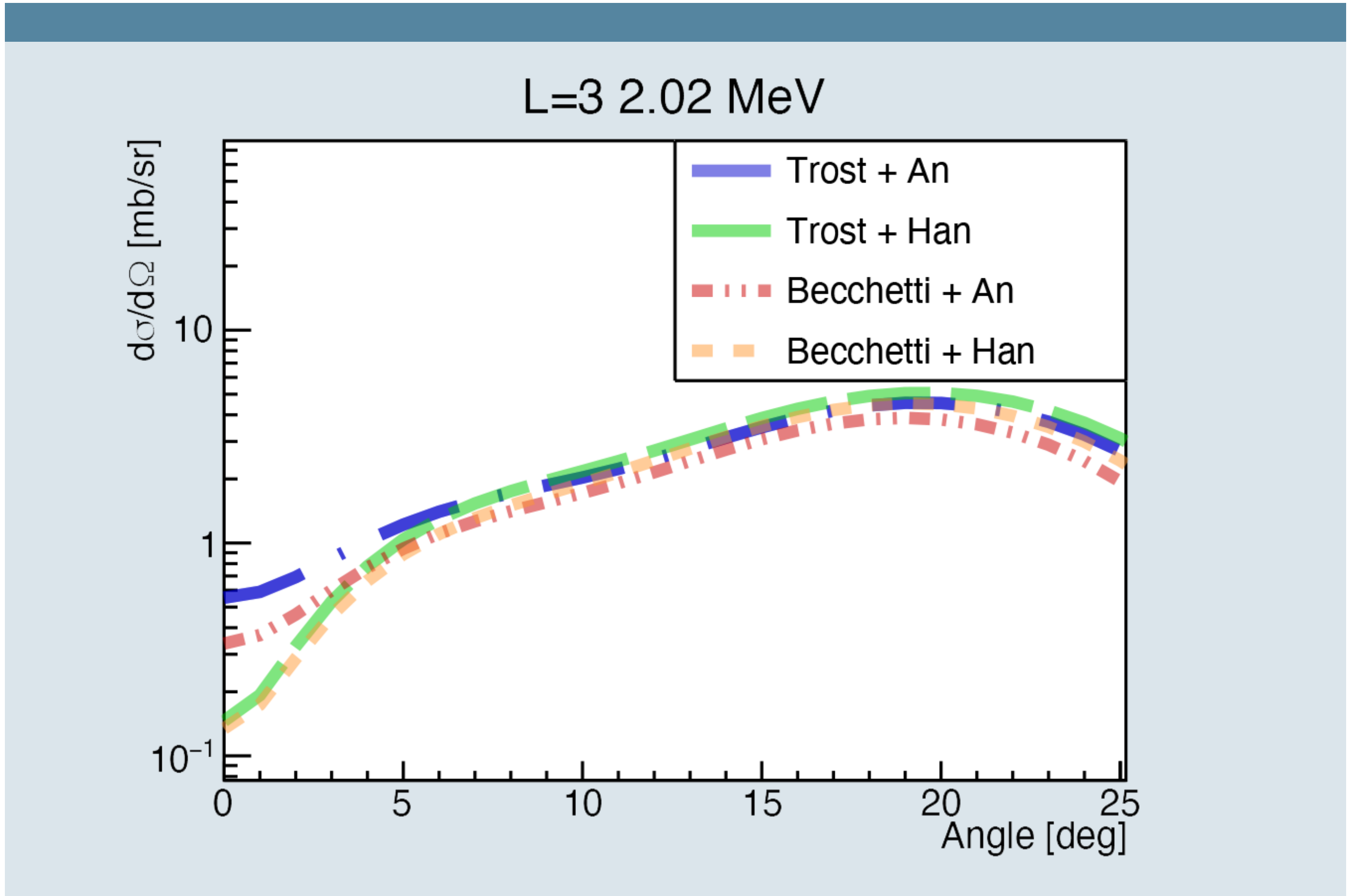

- Finite-range FRESCO calculation
- The position of the maxima of the distributions is affected minimally by the optical potential choice
- These calculations are the input for the Geant4 Monte Carlo simulations

Overlaps for cross section calculations

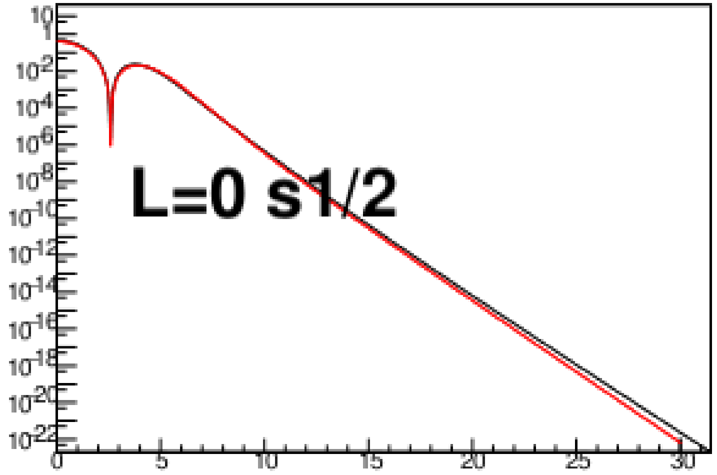

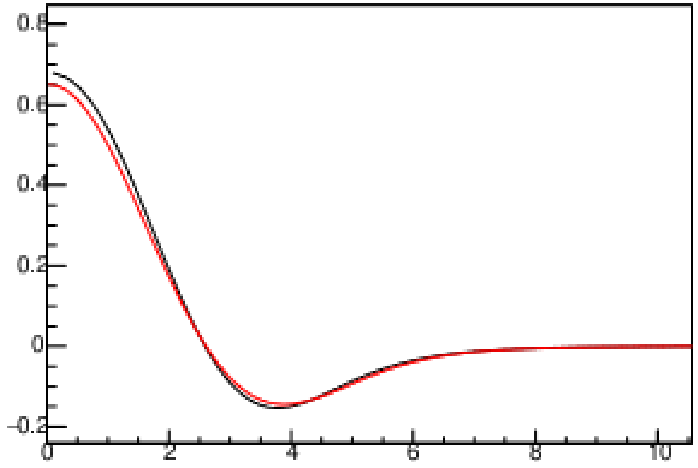

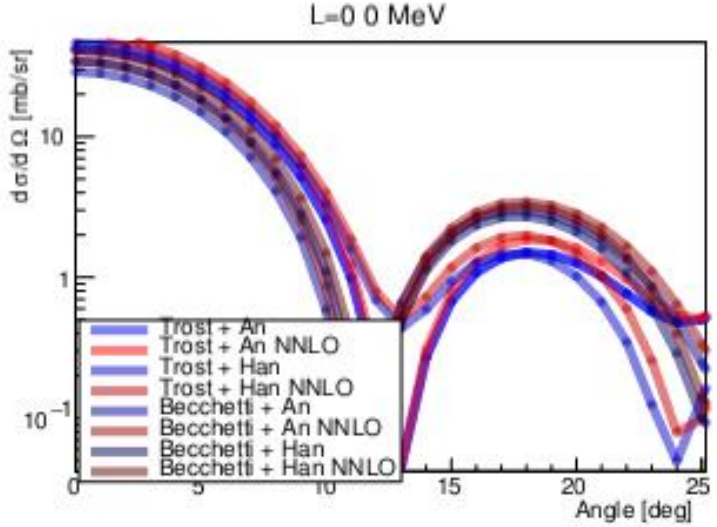

- Overlap from ab-initio and WS similar
- Difference possible in case of halo orbitals ?

Results

Particle spectra from MUGAST-VAMOS coinc.

- Optical potential tested on ^{48}Ca(d, ^{3}He)^{47}K data

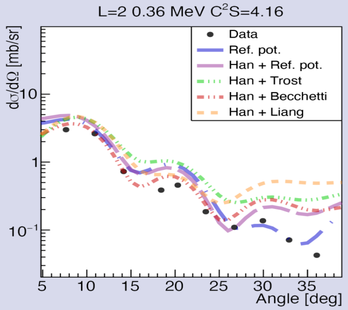

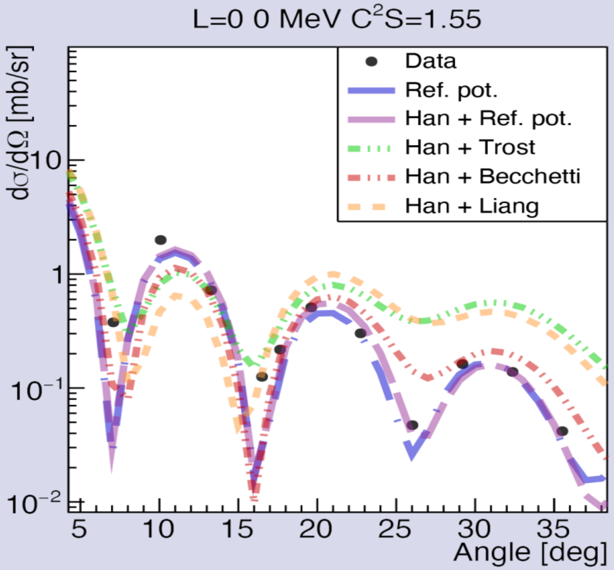

- Elastic scattering of the ^{47}K(d,d)^{47}K reaction

  @ 7.52 MeV/u:
  tested on recent data acquired with the same setup [Paxman, C. and the e793s collaboration. Priv. Comm]

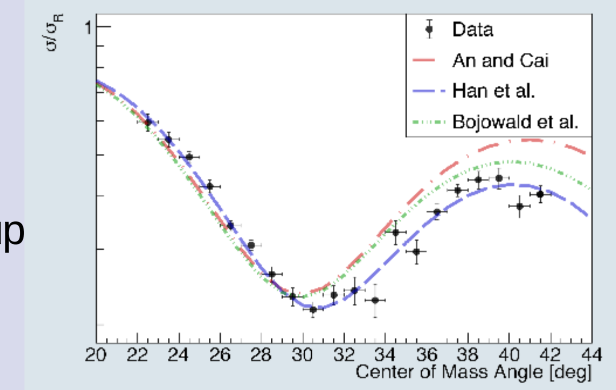

Spectroscopic factors

The SM (SDPF-U) fails the comparison with experimental data in terms of C^2S.

C²S[L]/C²S[L = 0]	3/2⁺ state	7/2⁻ state
SDPF-U	0.63	2.6
Experiment	$0.10^{+0.11}_{-0.10}$	$1.10^{+0.18}_{-0.15}$

- **$\pi s_{1/2}$ empty, $\pi d_{3/2}$ full !**
- The proton WF of the g.s. of ^{46}Ar is not correctly described

Results

Particle spectra from MUGAST-VAMOS coinc.

- Optical potential tested on ^{48}Ca(d, ^{3}He)^{47}K data

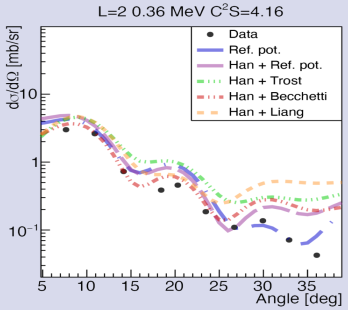

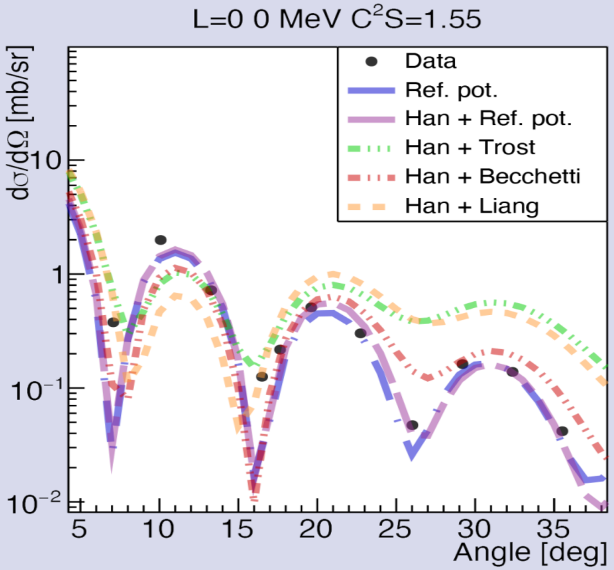

- Elastic scattering of the ^{47}K(d,d)^{47}K reaction @ 7.52 MeV/u: tested on recent data acquired at the same setup [Paxman, C. and the e793s collaboration. Priv. Comm]

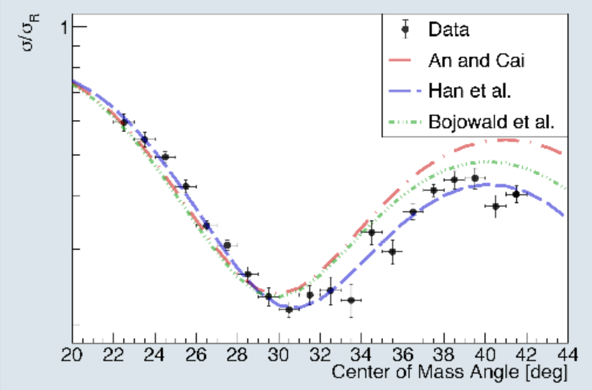

Spectroscopic factors

The SM (SDPF-U) fails the comparison with experimental data in terms of C^2S.

$C^2S[L]/C^2S[L=0]$	$3/2^+$ state	$7/2^-$ state
SDPF-U	0.63	2.6
Experiment	$0.10^{+0.11}_{-0.10}$	$1.10^{+0.18}_{-0.15}$

- **$\pi s_{1/2}$ empty, $\pi d_{3/2}$ full !**
- The proton WF of the g.s. of ^{46}Ar is not correctly described

Result sensitivity to optical potentials (I)

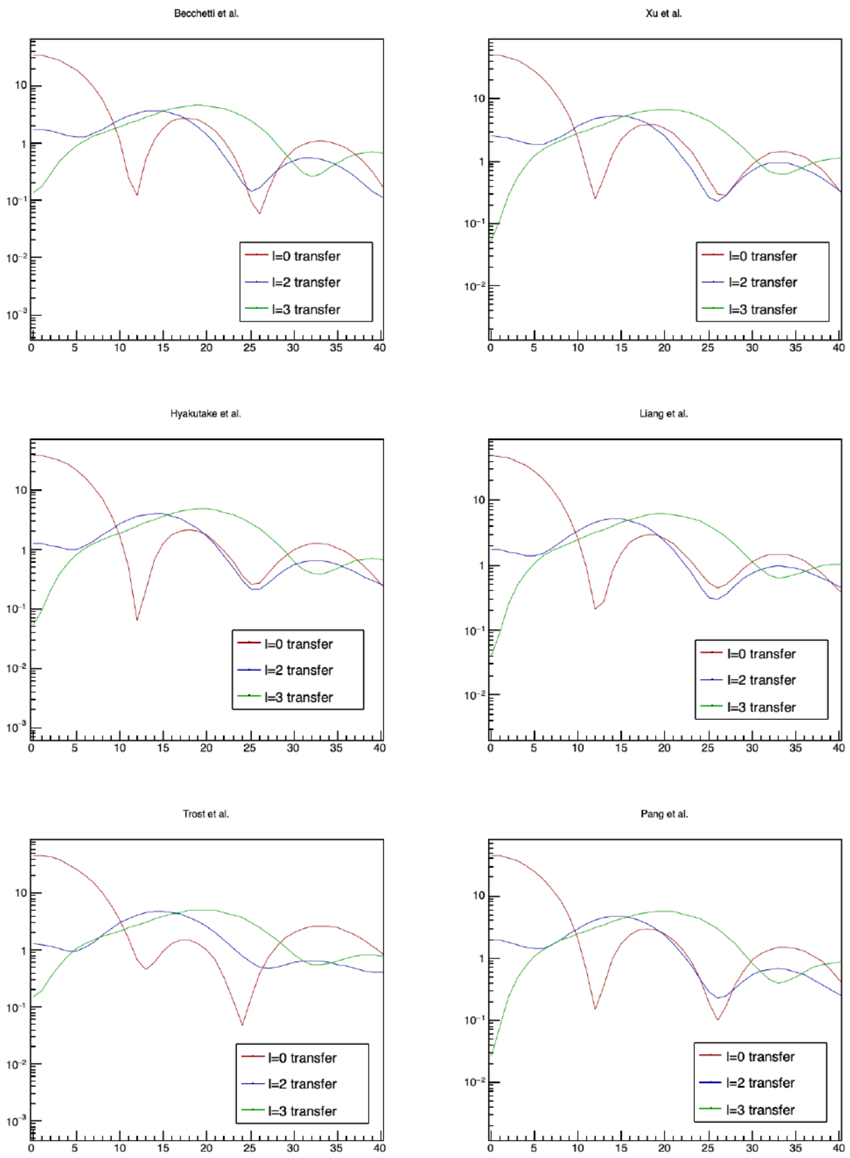

- Absolute cross sections are sensitive to the chosen optical potential
- Relative (ratio of) cross sections much less sensitive

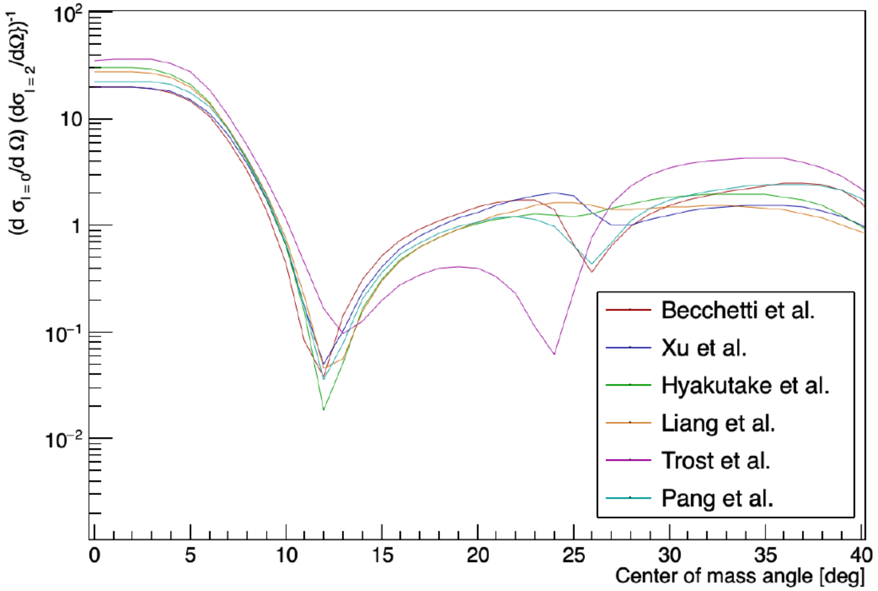

Results sensitivity to optical potentials (II)

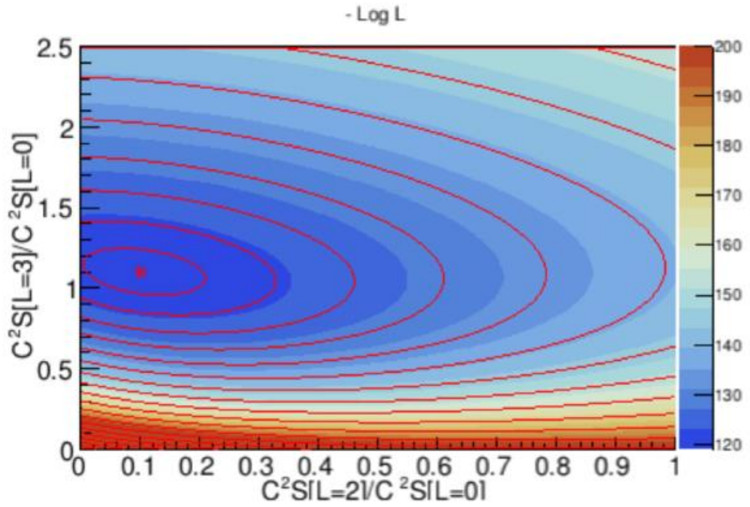

Becchetti et al.

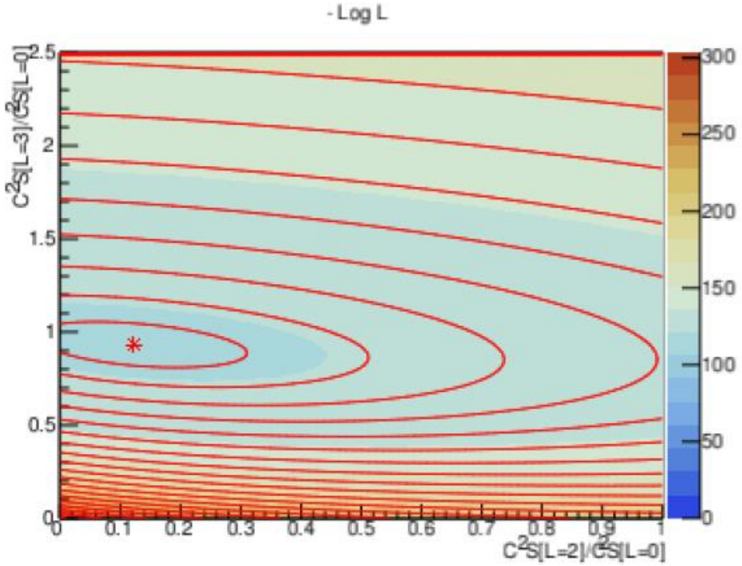

Xu et al.

Ab-initio model NNLO$_{sat}$: shell structure

Ab-initio calculations

- Ab-initio calculations with the NNLOsat in ADC2 and ADC3
  (C. Barbieri, S. Brolli, V. Somà)
- NNLO$_{SAT}$ chosen because of its capability of reproducing radii (cross check with the NNLO$_{lnl}$ in ADC2)
- 14 harmonic oscillator shells and $\hbar\Omega$=22 MeV to optimize the convergence of binding energies
- BE and charge radii well in agreement with ^{48}Ca and ^{46}Ar data
- **SF in ^{46}Ar in agreement with data**

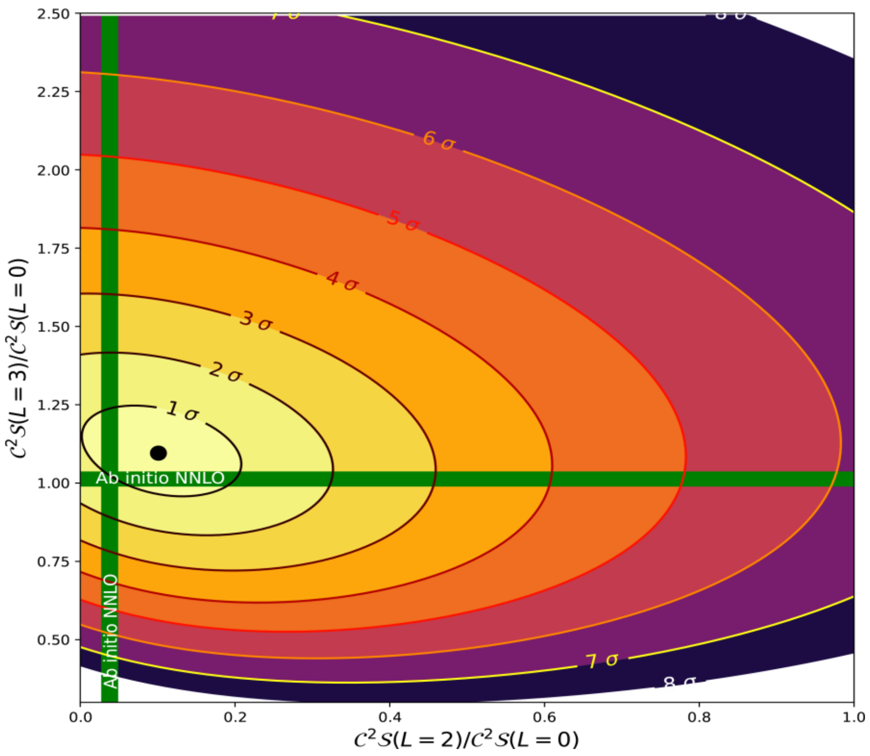

- NNLO$_{SAT}$: a $\pi d_{3/2}$ subshell closure and an empty $\pi s_{1/2}$

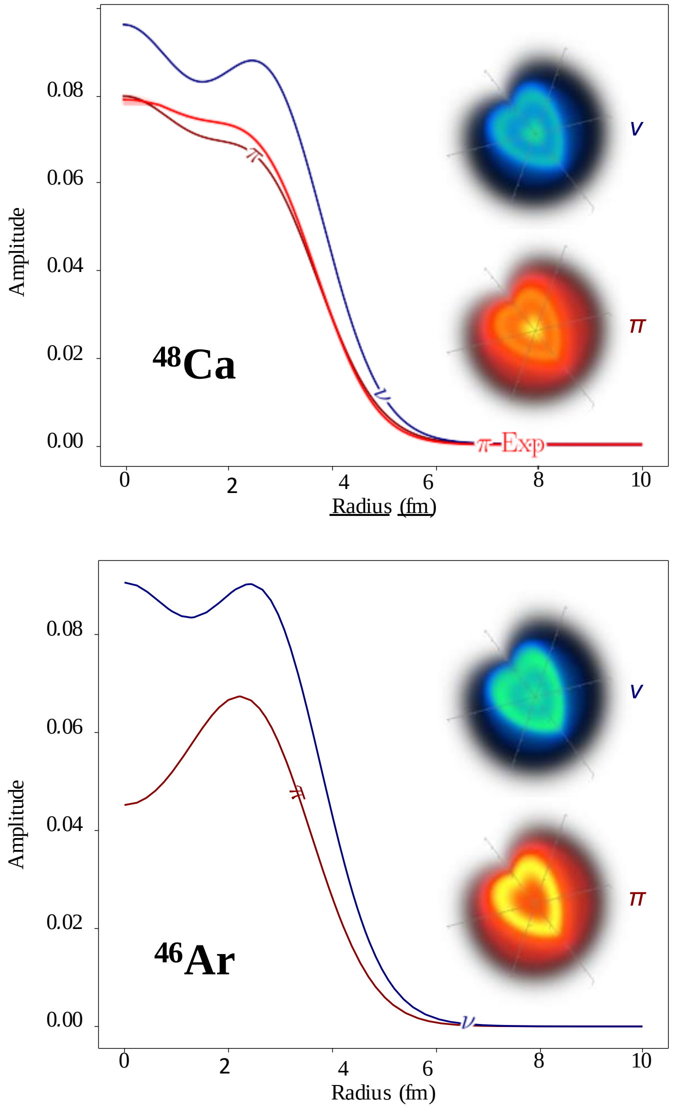

And the B(E2) ?

B(E2) puzzle solved ?

- Naive considerations: by closing the $d_{3/2}$ shell the restricted proton space will return a small B(E2) –> confirmed by SM calculations
- Mapping the NNLOsat χEFT Hamiltonian into the effective mean-field orbits generated by SCGF ADC(3)

  Phys. Rev. C 100, 024,317 (2019)
- The Hamiltonian was then diagonalized, with Antoine adjusting SP energies to reproduce experimental ^{46}Ar, ^{47}K level schemes:

  $B(E2, 2^+ \rightarrow 0^+) = 30\ e^2fm^4$

Radii, bubble, island of inversion: a link ?

- large charge and matter radii in $^{50-52}$Ca
- island of inversion at N=28
- central charge density depletion in ^{46}Ar

A link ?

A speculation

- $\nu p_{3/2} \nu p_{1/2} \nu f_{5/2}$ neutrons displacing matter from the center of the nucleus because of oversaturation
- In Ca isotopes, the Z=20 shell closure prevents protons from moving away from the core, which then has to swell

Large radii in $^{50-52}$ca

?

- $\nu p_{3/2}$ occupied by one neutron across N=28 in ^{46}Ar due to Island of inversion approaching -> oversaturation
- In ^{46}Ar, protons can move between $\pi s_{1/2}$ and $\pi d_{3/2}$

$\pi s_{1/2}$ depletion in ^{46}Ar-^{44}S…

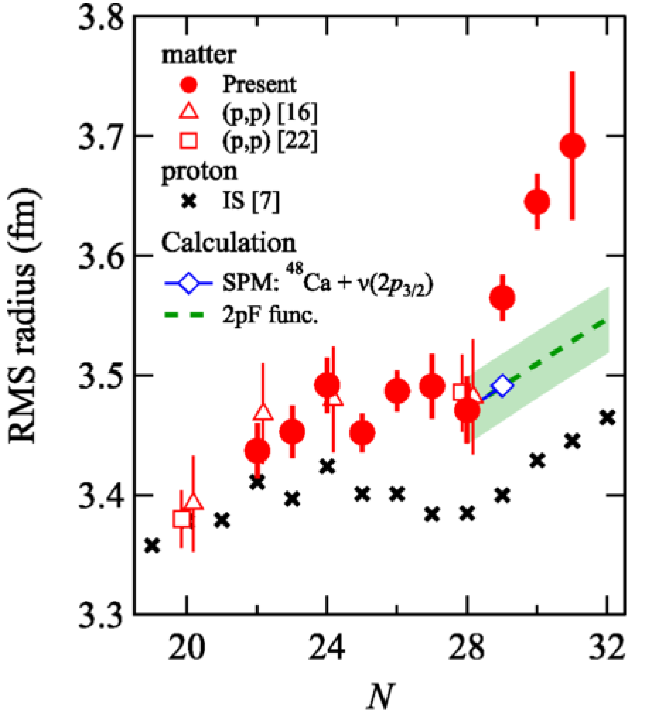

Phys. Rev. Lett. 124, 102501 (2020)

Nat. Phys. 12, 594–598 (2016)

Future developments

A new ^{3,4}He cryotarget: CTADIR

CTADIR

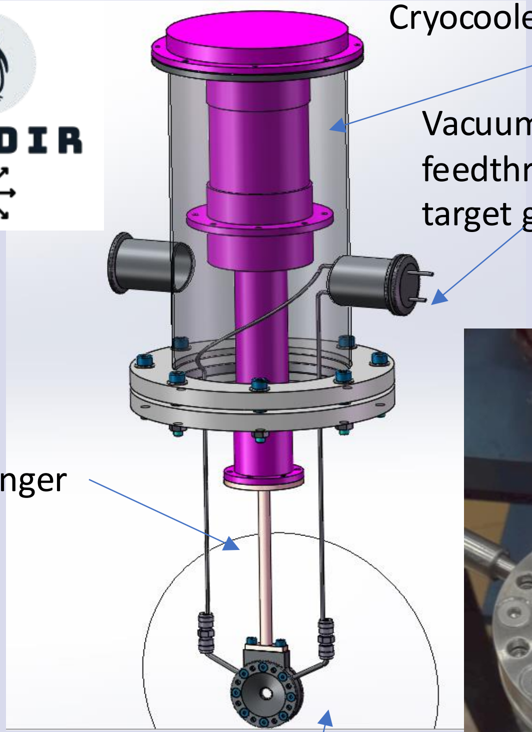

PRIN

A 4π DSSD: GRIT

- GRIT designed to be coupled with AGATA and CTADIR

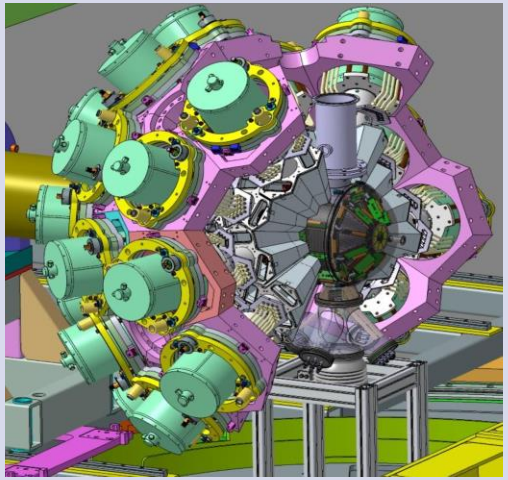

- AGATA campaign at LNL ongoing, direct reactions in the future

CONCLUSIONS

- Evidence of charge density depletion along N=28 below ^{48}Ca: the case of ^{46}Ar
- Direct proton transfer reactions with cryogenic targets as ideal tools to explore the shell structure linked to saturation properties
- $\pi s_{1/2}$ depletion in ^{46}Ar linked to shell evolution: other density "bubbles" to be expected in exotic nuclei → electron scattering on unstable beams
- Improved tools for direct reactions
- Can ab-initio optical potentials and overlaps be tested against measured elastic scattering ? Observable to detect halo orbitals ?

Collaboration

Experimentalists:

Daniele Brugnara, Andrea Gottardo, Marlene Assié, Daniele Mengoni, Antoine Lemasson, S. Bottoni, Emmanuel Clement, Freddy Flavigny, Diego Ramos, Franco Galtarossa, Adrien Matta, Valerian Girard-Alcindor,

Mathieu Babo, Dino Bazzacco, Didier Beaumel, Yorick Blumenfeld, Ushasi Datta, Giacomo de Angelis, Gilles de France, Jérémie Dudouet, Jose Duenas, Alain Goasduff, Eleonora Gregor, Fairouz Hammache, Andrés Illana, Louis Lalanne, Sylvain Leblond, Ivano Lombardo, Naomi Marchini, Bénédicte Million, Francesco Recchia, Kseniia Rezynkina, Marco Rocchini, Jennifer Sanchez Rojo, Marco Siciliano, Josè Javier Valiente-Dobòn, Irene Zanon and Magdalena Zielinska

Theoreticians:

C. Barbieri, S. Brolli, G. Colò, V. Somà, E. Vigezzi

AND A GREAT THANK TO THE GANIL AND IJCLab ORSAY ENGINEERS and TECHINCAL STAFF !

THANK YOU FOR YOUR ATTENTION !

BACKUP SLIDES

A speculation on the speculation: how is N=28 formed ?

- N=28 is a non-HO magic number: spin-orbit or extruder-intruder ?

  E. Caurier, G. Martínez-Pinedo, F. Nowacki, A. Poves, and A. P. Zuker Rev. Mod. Phys. **77**, 427 – Published 16 June 2005

- Is really 3-body force the origin of the $f_{7/2}$ «self» binding ?

  A. P. Zuker, Phys. Rev. Lett. **90**, 042502 (2003)

- Or maybe is the unbinding of the $p_{3/2}p_{1/2}$ shells (halo-like) to create the N=28 magic number ?

  J. Bonnard and A. P. Zuker 2018 *J. Phys.: Conf. Ser.* **1023** 012016

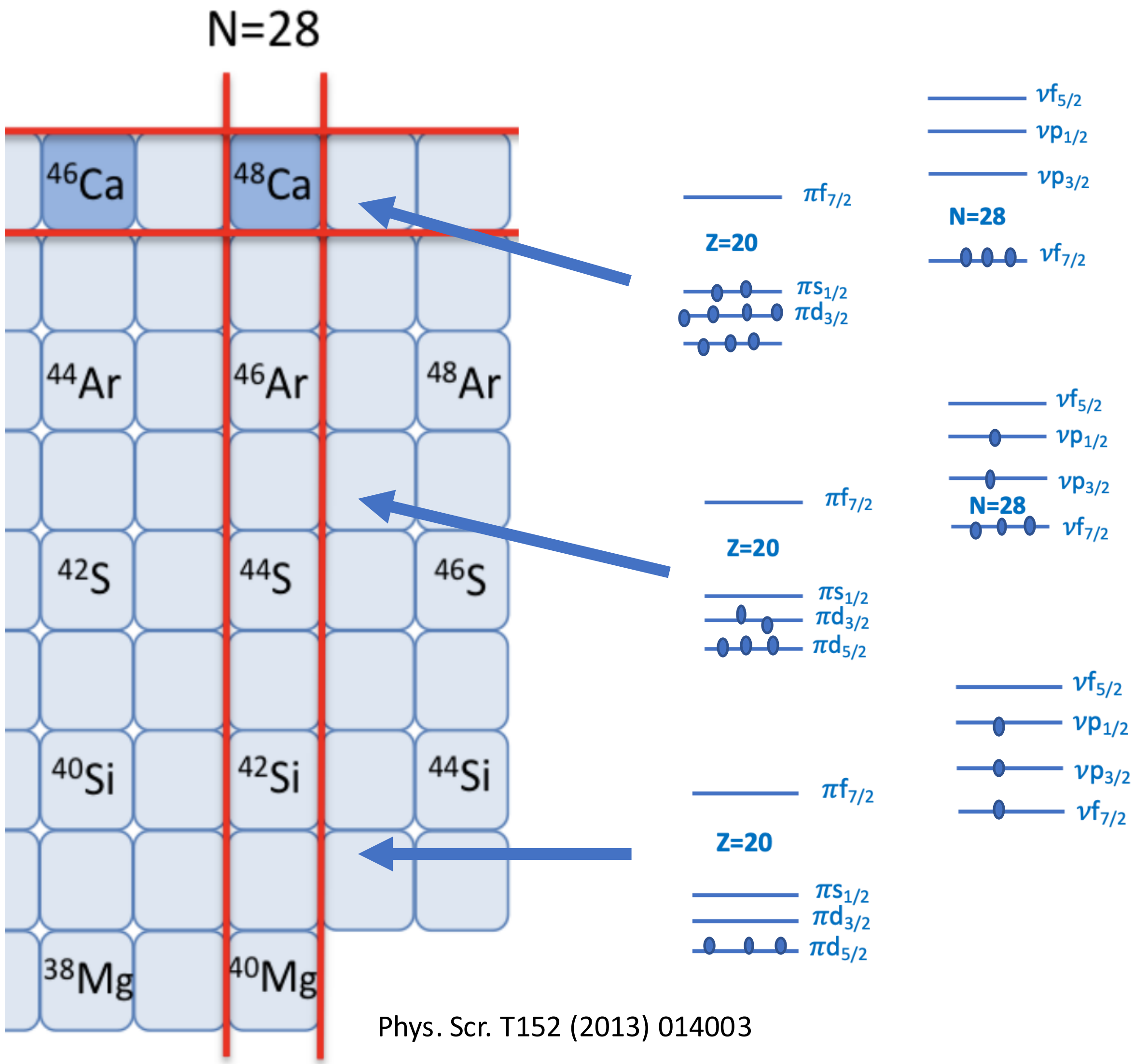

Phys. Scr. T152 (2013) 014003

Ab-initio model NNLO$_{sat}$

^{46}Ar magic ?

- *3-point mass difference:*
  $\Delta^{(3)} = -\frac{1}{2}[B(^{47}K)-2B(^{46}Ar)+B(^{45}Cl)]$
- $\Delta^{(3)}_{\mathrm{EXP}}$= 4.830 MeV
- $\Delta^{(3)}_{\mathrm{NNLO_{SAT}}}$= 2.766 MeV
- In ^{46}Ar: $2\Delta^{(3)}$ = energy gap among a full $\pi d_{3/2}$ and an empty $\pi s_{1/2}$
- Large energy gap among proton shells in ^{46}Ar

$$\frac{d\sigma_k}{d\Omega} = g\,\mathcal{C}^2\mathcal{S}_k\,\frac{d\sigma_k^{SP}}{d\Omega}$$

$\pi d_{3/2} - \pi s_{1/2}$: a reciprocal chase

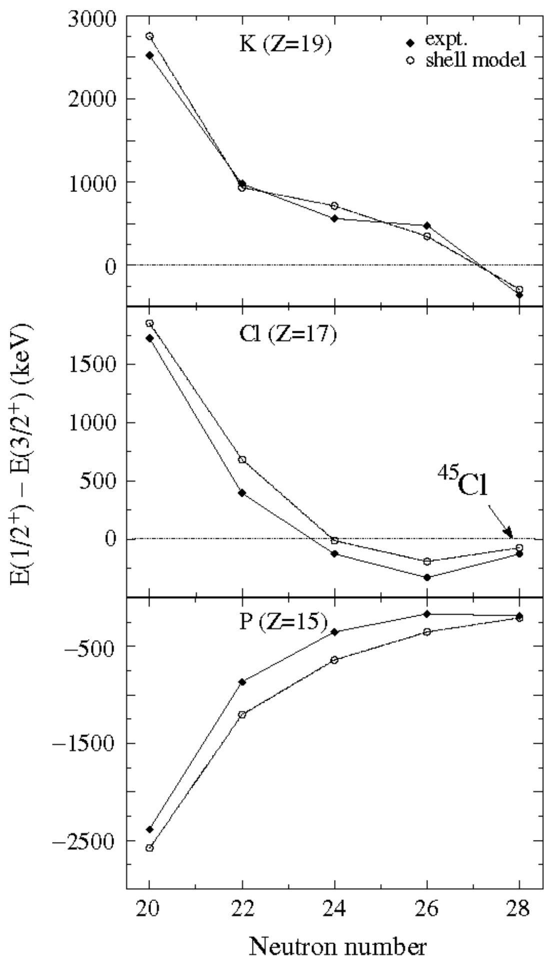

A. Gade et al., PRC 74, 034322 (2006)

S. R. Stroberg et al., PRC 86, 024321 (2012):

in ^{45}Cl $3/2^+$ is maybe the fundamental state (forbidden M1 strength)

A measurement of $\pi s_{1/2}$ depletion in ^{46}Ar will help

to assess a possible change in the $\pi s_{1/2}$- $\pi d_{3/2}$ positions

Is there a strong $\pi s_{1/2}$ depletion in ^{46}Ar ?

Central density depletion linked to spin-orbit splitting reduction

L. Gaudefroy et al. PRL 97, 092501 (2006)

Inverse kinematics: H and He cryogenic target density

For reference: σ = 1mbarn, beam = 10^4 pps, ^{2}H target= 1mg/cm^2

260 reactions/day, 1800 reactions/week

	H semisolid	^{3}He cryogenic
Atoms/cm^2	$4{\cdot}10^{20}$	$4{\cdot}10^{20}$
mg/cm^2	0.7	2.1
Thickness (mm)	0.1	3

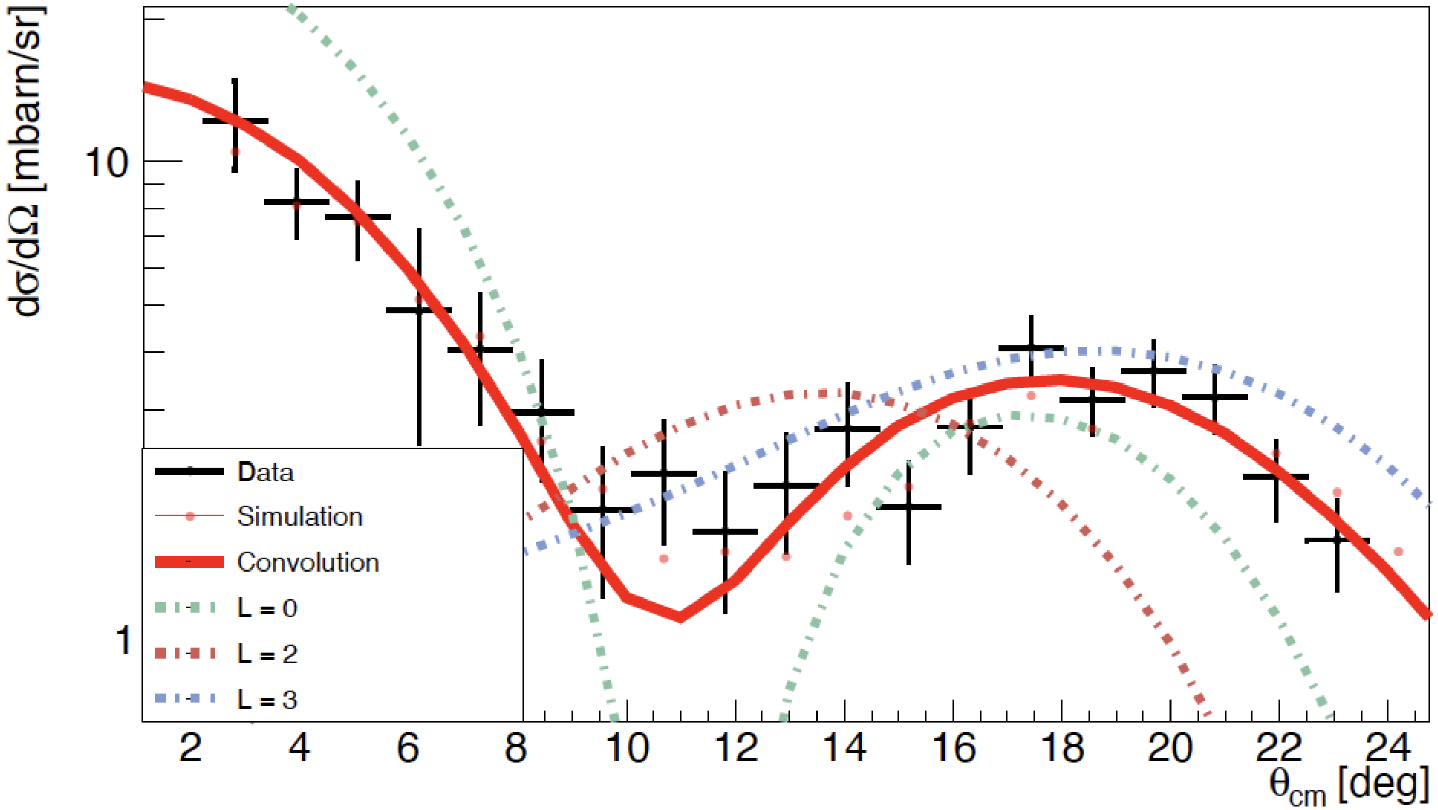

dσ/dΩ [mbarn/sr]
10
1
2
4
6
8
10
12
14
16
18
20
22
24
θcm [deg]
Data
Simulation
Convolution
L = 0
L = 2
L = 3

Neutron observables $= \Rightarrow$ D_n

$$D_N(Z, A) = (-1)^{N+1} [S_n(Z, A+1) - S_n(Z, A)]$$

D_n [Z. Meisel et al. PRL 114, 022501 (2015)]

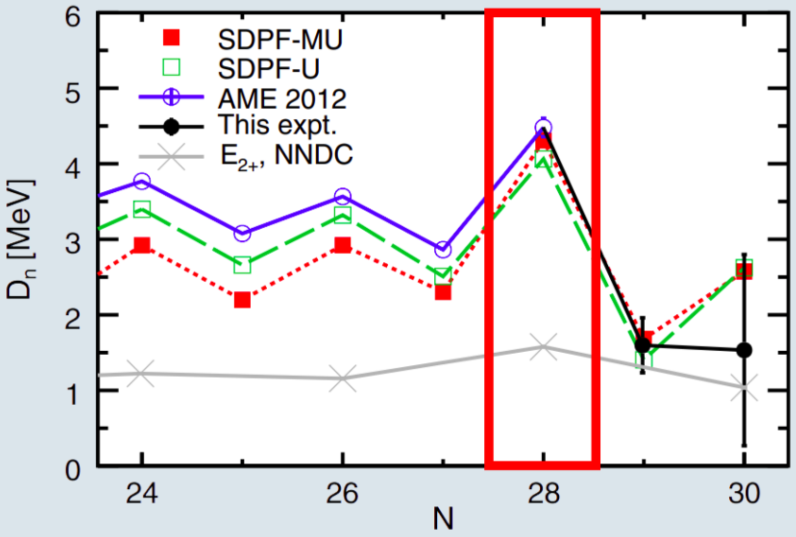

- Mass measurements confirm the N=28 shell closure in ^{46}Ar and its breakdown in the S isotopes (by observing a peaked value of D_n at N=28 with a sudden drop for more neutron-rich ^{46}Ar isotopes)
- **Experimental data and theory well in agreement** ($= \Rightarrow$ SDPF-U describes well the valence-core neutron interaction)

γ-rays in coincidence with ^{47}K in VAMOS

Response of AGATA with tagged ^{47}K

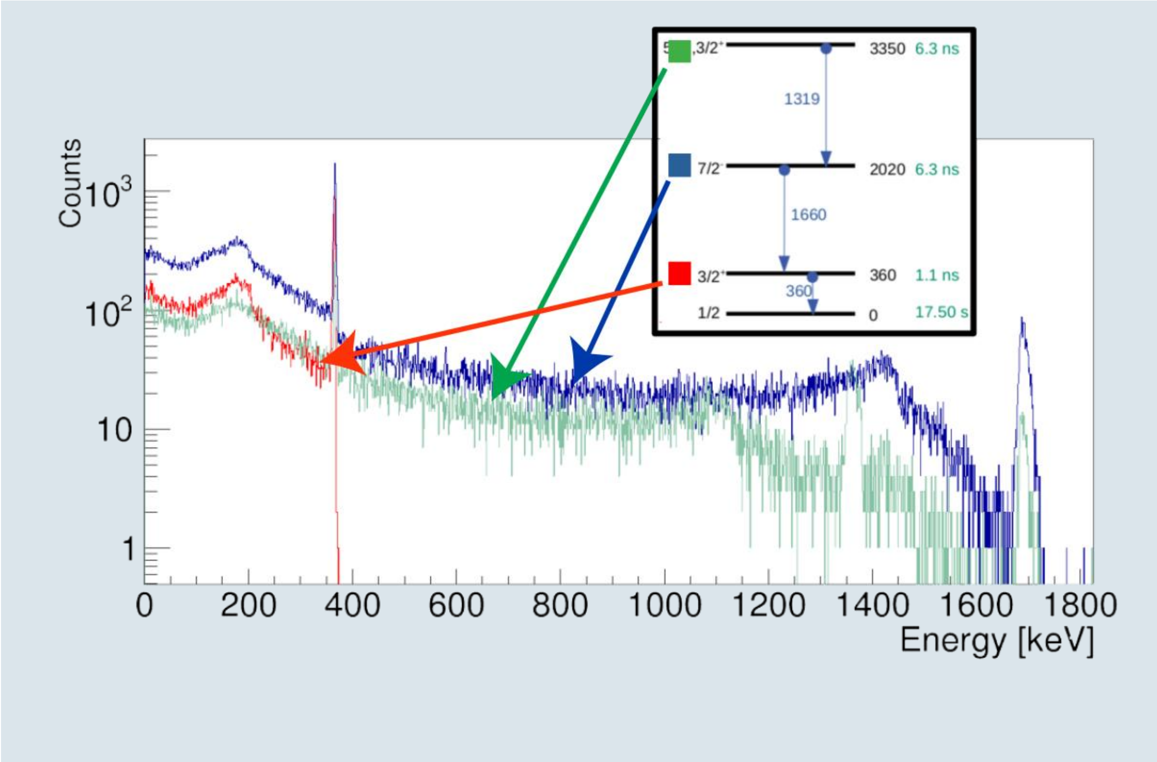

- AGATA is sensitive to the probability of populating different states
- Due to the long lifetime of the *f* 7/2 state, the efficiency of the spectrometer changes drastically
- γ rays at 360 keV are consistent with the direct population of the $7/2^-$ state

Experimental Setup : Beam tracker

CATS2 [Ottini-Hustache, S. et al., NIM A 431, 476 (1999)]

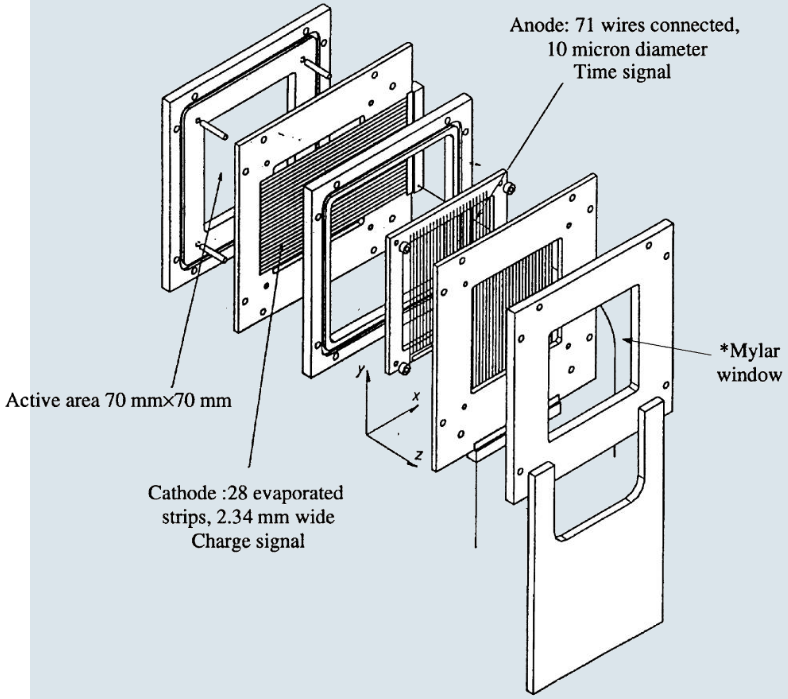

- Overall effective area of (70 × 70) mm^2
- Can withstand up to 10^6 pps
- Timing information is obtained from the cathode with a resolution of 400 ps for the TOF selection of VAMOS and MUGAST
- Position resolution of < 0.5 mm
- One detector present and located 2 m before the target position

AGATA: calibration

Hit pattern of the 39 crystals

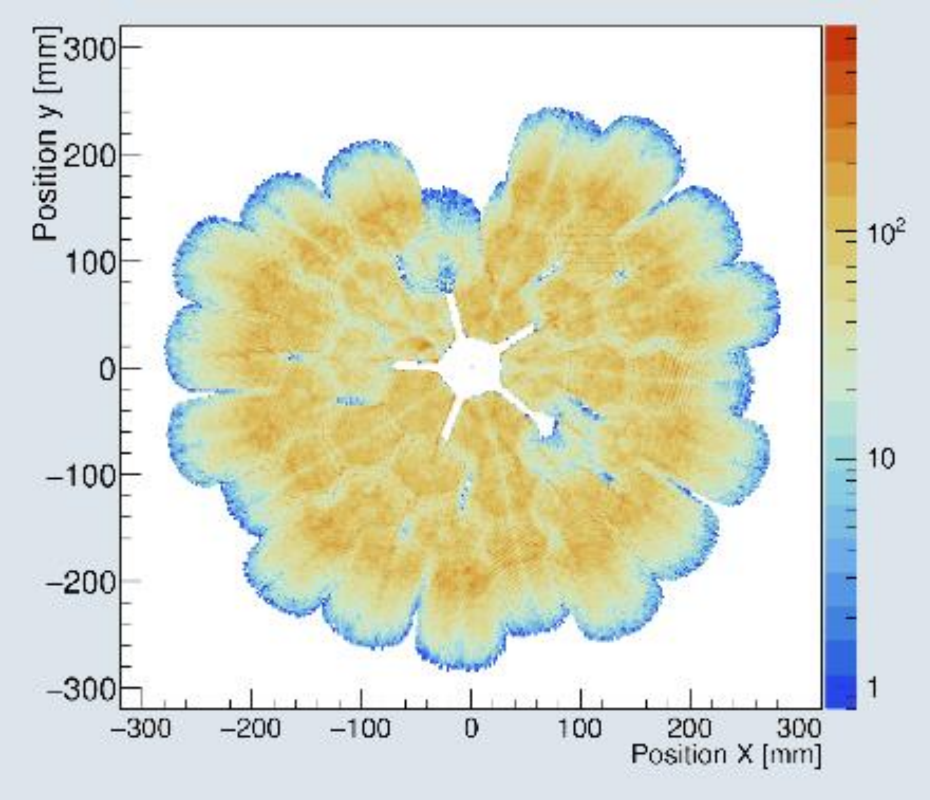

^{152}Eu calibration

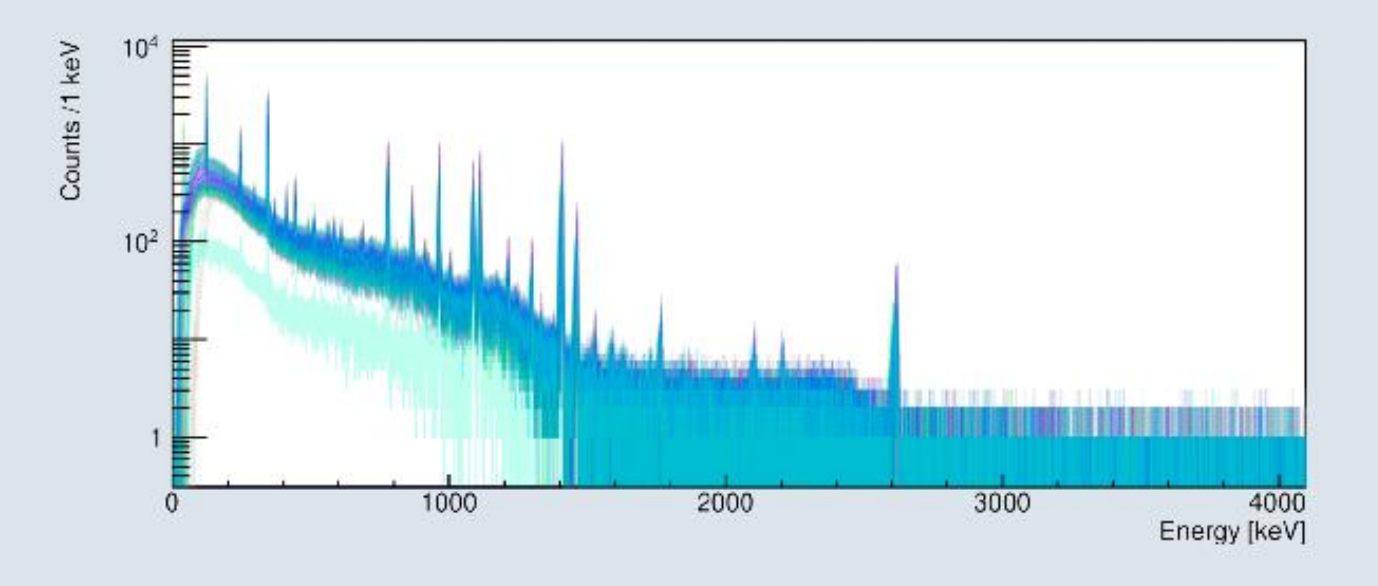

The ^{46}Ar(^{3}He,*pn*)^{47}K reaction

- The weakly bound deuteron can breakup after the transfer of the proton
- This reaction is a three-body reaction, as a consequence no kinematic line is present
- Since the resolution in ϕ of VAMOS is limited, and/or the neutron is not detected, it is impossible to reconstruct the kinematics
- Nevertheless, the γ-rays are detected by AGATA

^{47}K in VAMOS and ^{1}H in MUGAST

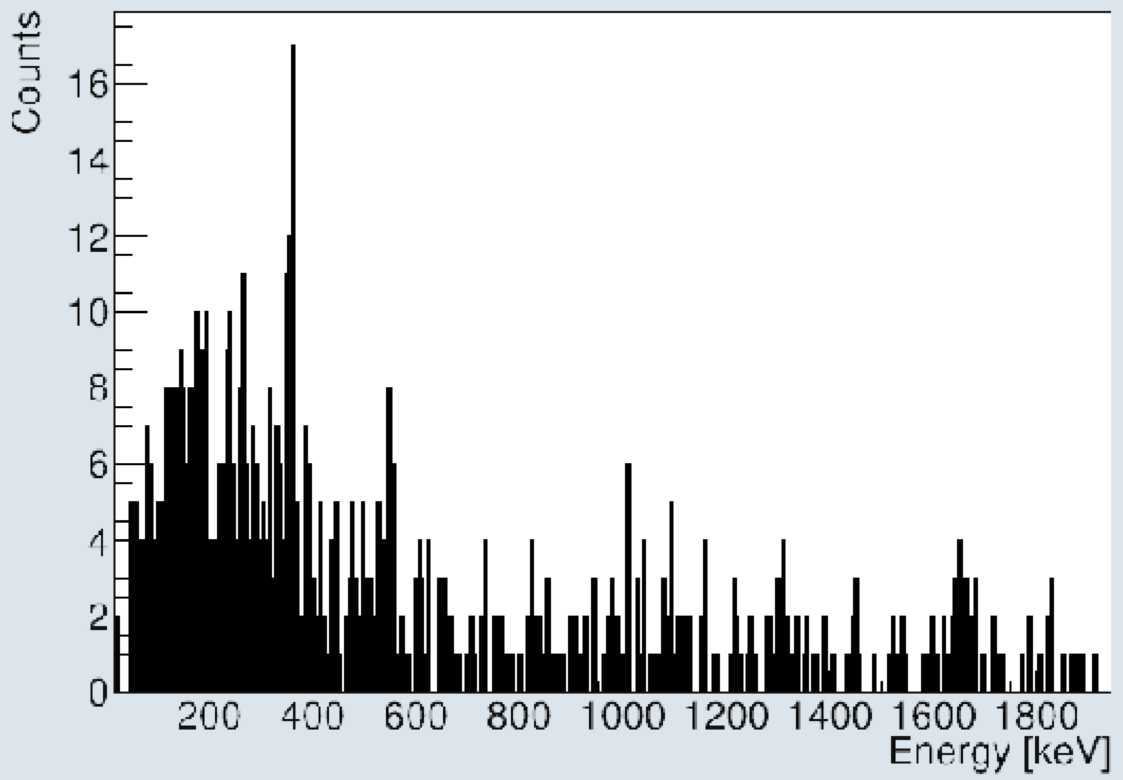

^{3}He equation of state: experimental data

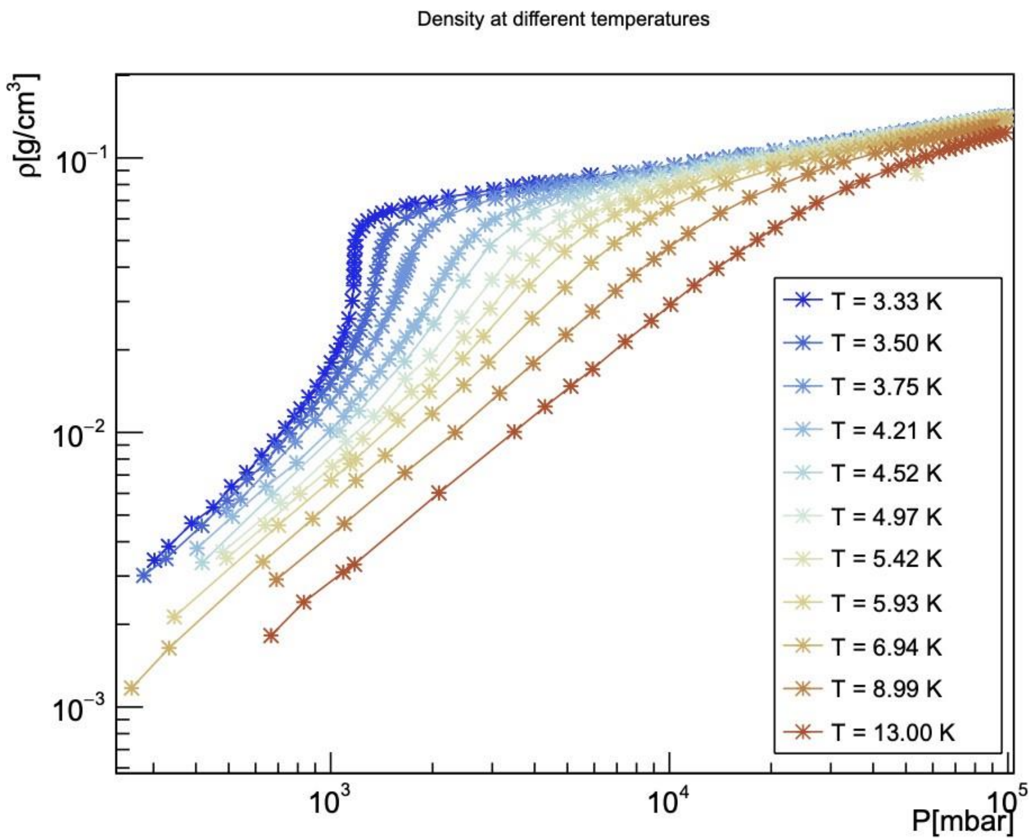

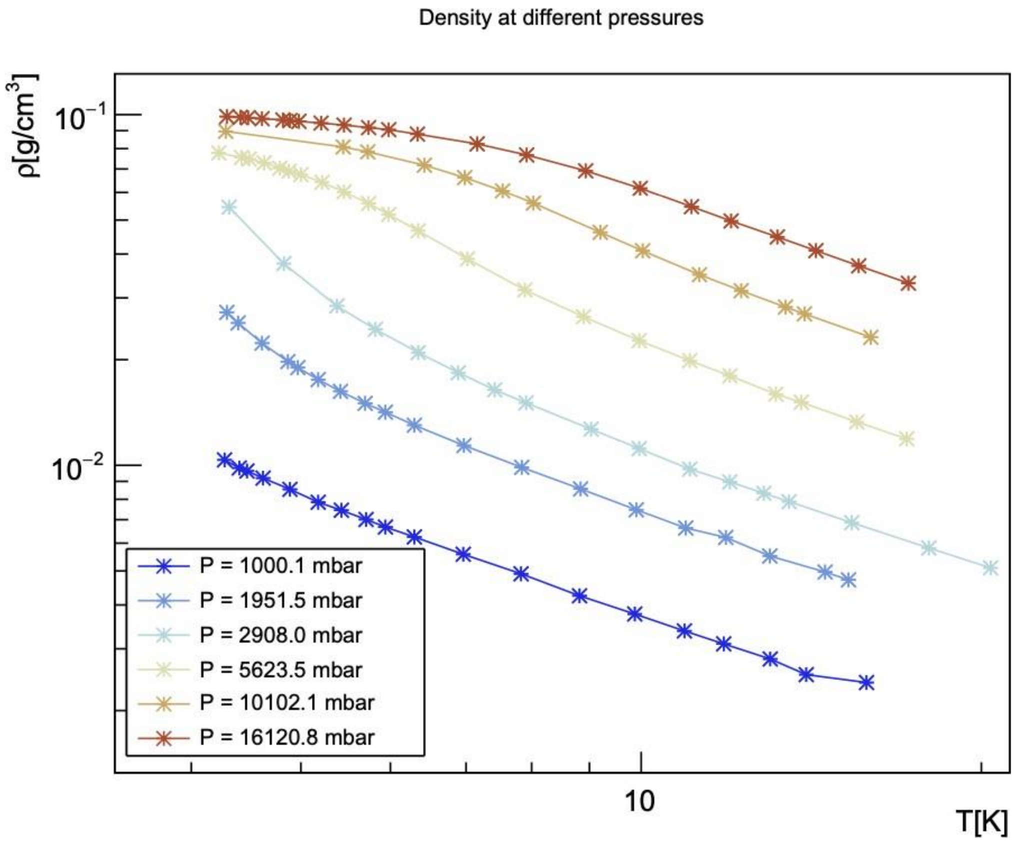

The onset of deformation in ^{44}S

- Mean field potential energy surfaces computed in the Hartree–Fock–Bogolyubov framework as a function of the deformation parameter [Rodr´ıguez-Guzm´an et al., PRC 65, 024304 (2002)]
- The evolution along the N = 28 shell closure indicates a quick onset of deformation along the neutron rich side.

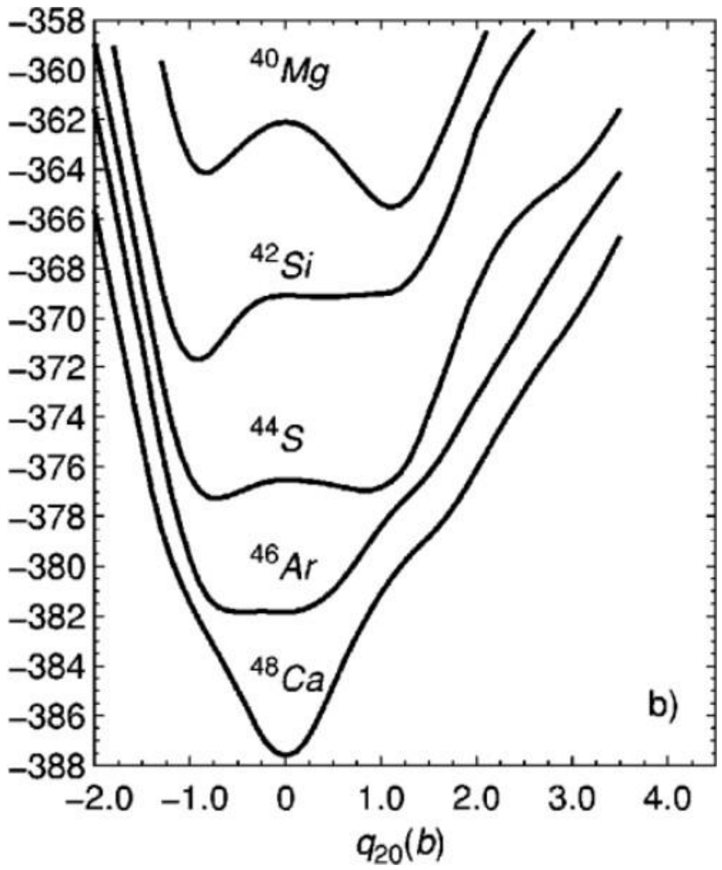

The optical potential

$$V(r) = V_R(r) + V_{SO}(r) + V_C(r) + i\,[W_D(r) + W_S(r) + W_{SO}(r)]$$

- The terms consist in the Coulomb potential V_c, the real (imaginary) part of the potential well V_r (W_S), the real (imaginary) spin-orbit component V_{SO} (W_{SO}) and the surface absorption W_D.

$$V_R(r) = -\frac{V_R(E)}{1 + \exp\left(\frac{r-R_R}{a_R}\right)} \qquad W_D(r) = -4W_D(E)\frac{\exp\left(\frac{r-R_D}{a_D}\right)}{\left[1 + \exp\left(\frac{r-R_D}{a_D}\right)\right]^2}$$

$$V_{SO}(r) = -\left(\frac{\hbar}{m_\pi c}\right)^2 (\vec{L}\cdot\vec{S})\,\frac{V_{SO}}{a_{SO}\,r}\,\frac{\exp\left(\frac{r-R_{SO}}{a_{SO}}\right)}{\left[1 + \exp\left(\frac{r-R_{SO}}{a_{SO}}\right)\right]^2}$$

Ice layer uniformity

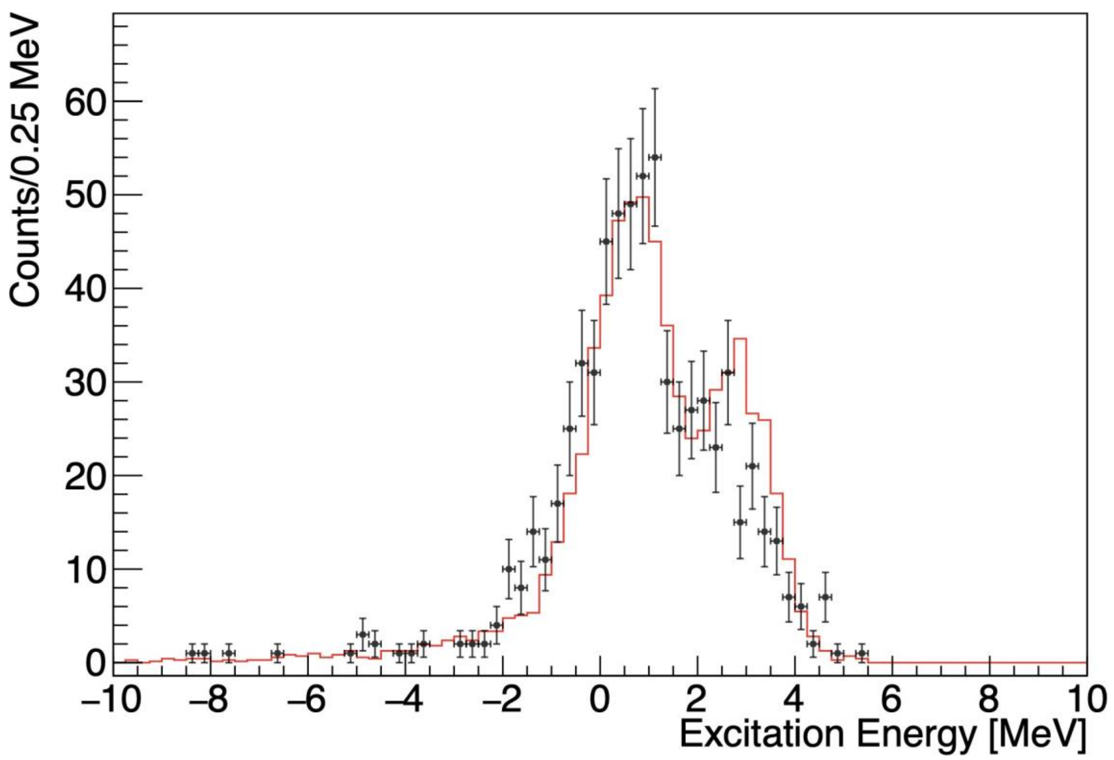

- Sampled from the Landau distribution

$$\Delta x = \frac{1}{\pi c}\int_0^\infty dt\, e^{-t} \cos\left(t\,\frac{x-\mu}{c} + \frac{2t}{\pi}\log\frac{t}{c}\right)$$

MUGAST: Simulation

NPTOOL [A Matta et al, J. Phys. G: Nucl. Part. Phys. 43 045113]

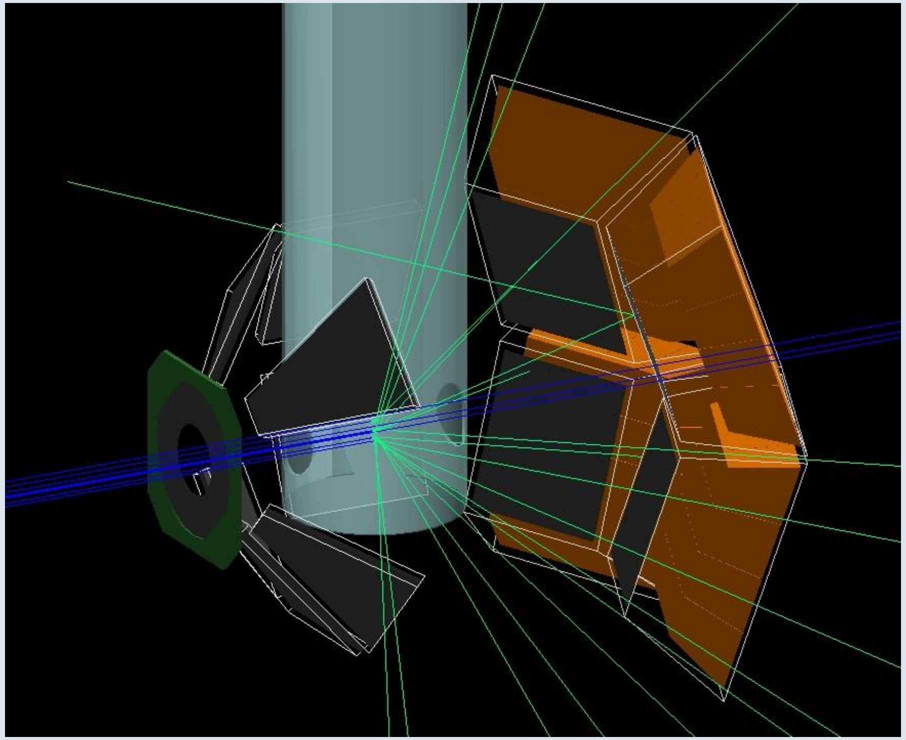

Accounts for:

- Ice growth over time on the windows
- Target deformation
- Missing strips
- Thresholds
- Dead layer
- VAMOS acceptance
- Charge state distribution
- Change in FRESCO calculations due to slightly varying mid-target energy
- *L* value transferred

AGATA: Simulation

- Geant4 simulation necessary to simulate response to feeding on 3/2 and 7/2, which have very dissimilar lifetimes
- It accounts for the reaction, the presence of the shadow created by the cryogenic target, the presence of the reaction chamber and the crystal intrinsic properties

AGATA [E. Farnea et al, NIM A 621 1 331-343] + HECTOR

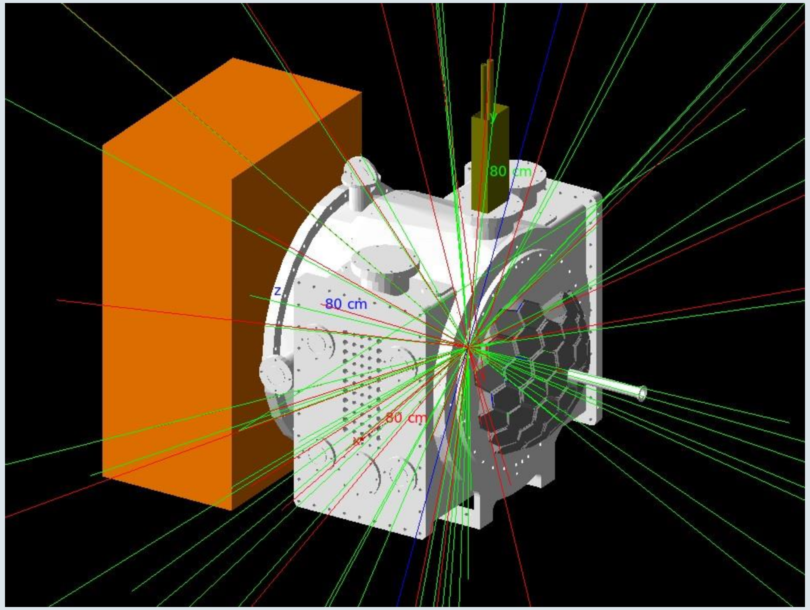

Simulation and source comparison

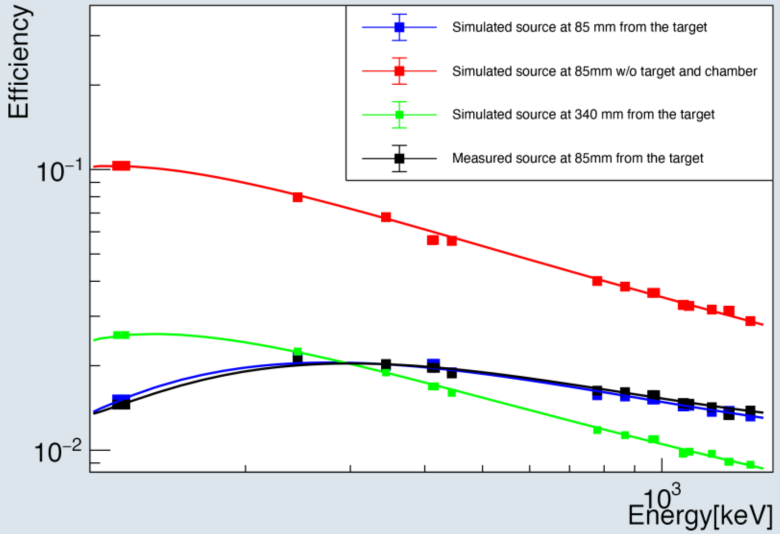

Angular distributions in the center of mass: comparison

Center of mass comparison with Fresco calculations

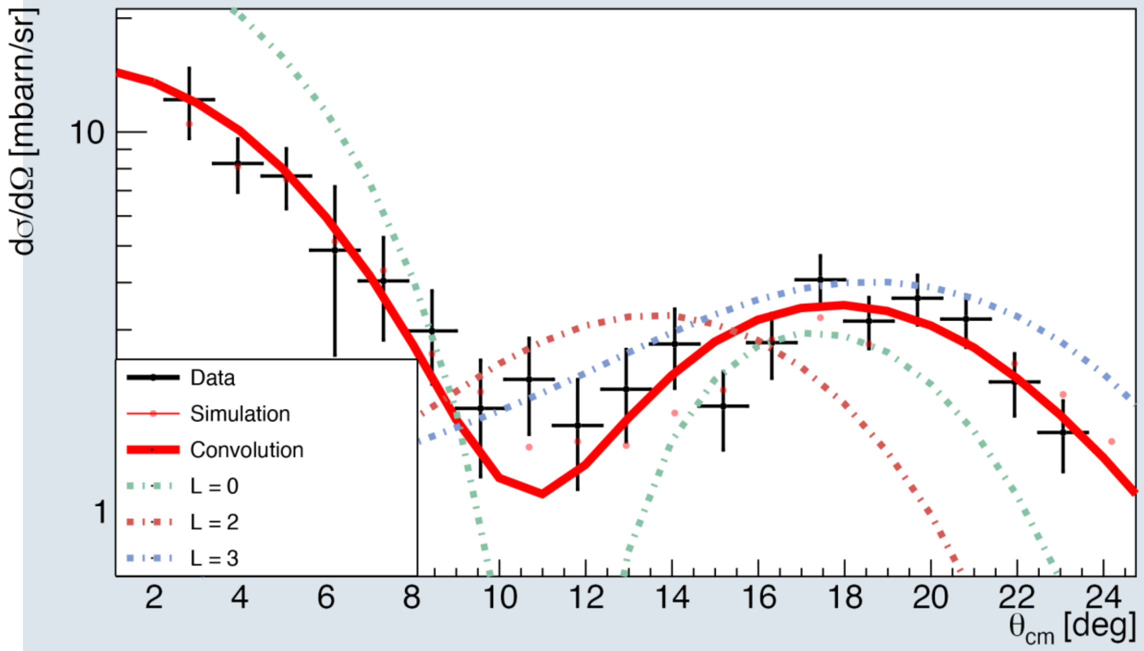

- The center of mass distribution, shows a remarkable agreement with the fit performed in the laboratory frame of reference.
- Different (global) optical potentials

  have little effect on the distributions at angles close to zero
- Different parametrizations of the optical potential return a compatible ratio of $C^2S[L = 2]/C^2S[L = 0]$

- **The peak of the $L = 2$ distribution is located in correspondence of the minimum of the overall distribution**

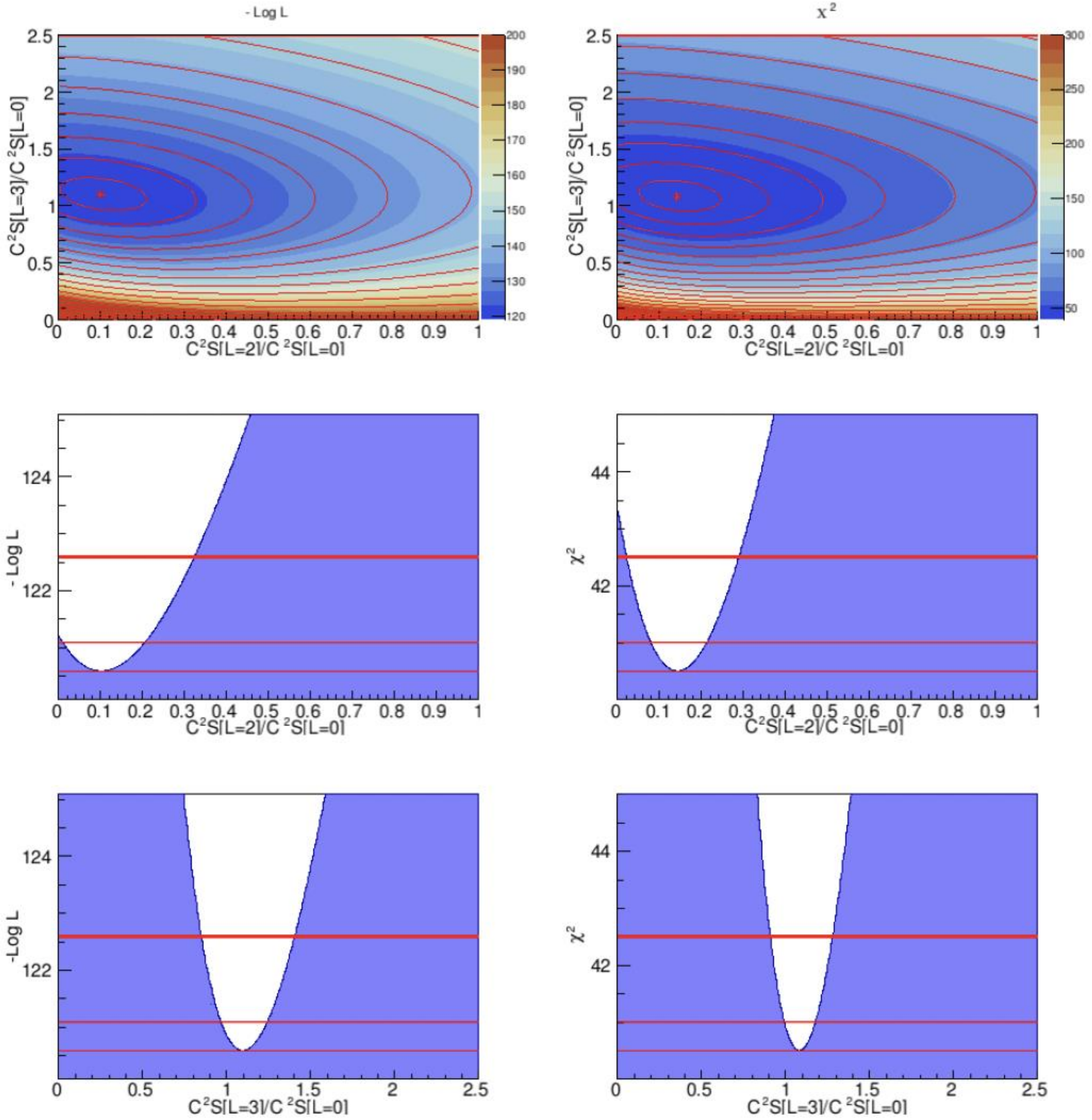

- Log L
χ^2
$C^2S[L=3]/C^2S[L=0]$
$C^2S[L=2]/C^2S[L=0]$
- Log L
χ^2
$C^2S[L=2]/C^2S[L=0]$
-Log L
χ^2
$C^2S[L=3]/C^2S[L=0]$

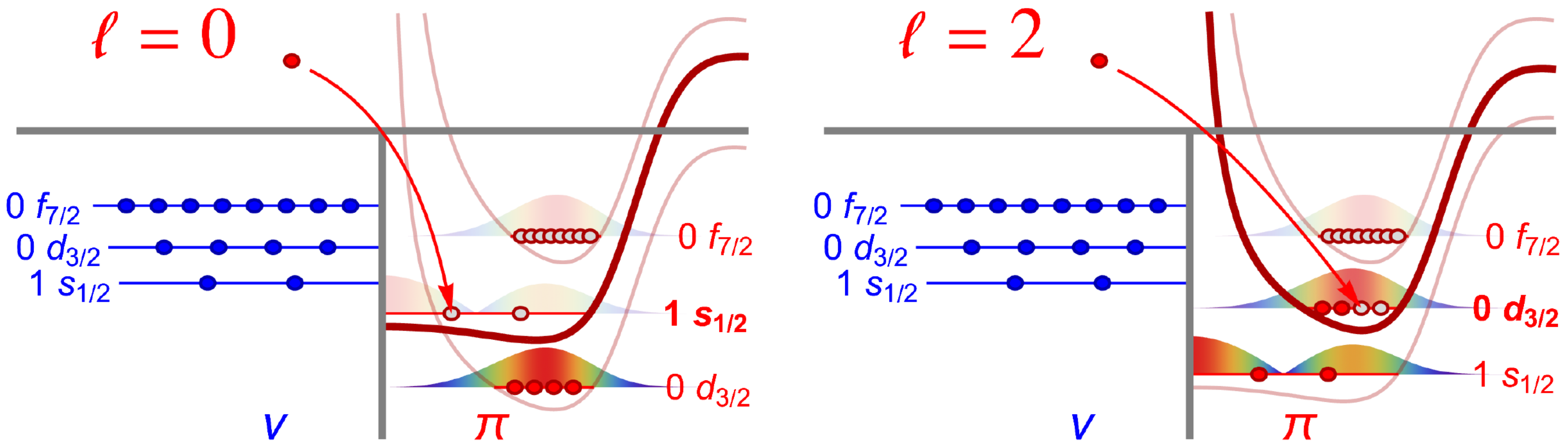

$\ell = 0$
0 $f_{7/2}$
0 $d_{3/2}$
1 $s_{1/2}$
ν
π
0 $f_{7/2}$
1 $s_{1/2}$
0 $d_{3/2}$
$\ell = 2$
0 $f_{7/2}$
0 $d_{3/2}$
1 $s_{1/2}$
ν
π
0 $f_{7/2}$
0 $d_{3/2}$
1 $s_{1/2}$